Available online at www.sciencedirect.com

ScienceDirect

Nuclear Physics B 898 (2015) 563–604

NUCLEAR PHYSICS B

www.elsevier.com/locate/nuclphysb

QCD corrections to $B \to \pi$ form factors from light-cone sum rules

Yu-Ming Wang [a,*], Yue-Long Shen [b]

[a] *Physik Department T31, Technische Universität München, James-Franck-Straße 1, D-85748 Garching, Germany*
[b] *College of Information Science and Engineering, Ocean University of China, Qingdao, Shandong 266100, PR China*

Received 8 June 2015; received in revised form 7 July 2015; accepted 14 July 2015

Available online 26 July 2015

Editor: Tommy Ohlsson

Abstract

We compute perturbative corrections to $B \to \pi$ form factors from QCD light-cone sum rules with B-meson distribution amplitudes. Applying the method of regions we demonstrate factorization of the vacuum-to-B-meson correlation function defined with an interpolating current for pion, at one-loop level, explicitly in the heavy quark limit. The short-distance functions in the factorization formulae of the correlation function involves both hard and hard-collinear scales; and these functions can be further factorized into hard coefficients by integrating out the hard fluctuations and jet functions encoding the hard-collinear information. Resummation of large logarithms in the short-distance functions is then achieved via the standard renormalization-group approach. We further show that structures of the factorization formulae for $f_{B\pi}^{+}(q^2)$ and $f_{B\pi}^{0}(q^2)$ at large hadronic recoil from QCD light-cone sum rules match that derived in QCD factorization. In particular, we perform an exploratory phenomenological analysis of $B \to \pi$ form factors, paying attention to various sources of perturbative and systematic uncertainties, and extract $|V_{ub}| = \left(3.05^{+0.54}_{-0.38}|_{\rm th.} \pm 0.09|_{\rm exp.}\right) \times 10^{-3}$ with the inverse moment of the B-meson distribution amplitude $\phi_B^{+}(\omega)$ determined by reproducing $f_{B\pi}^{+}(q^2 = 0)$ obtained from the light-cone sum rules with π distribution amplitudes. Furthermore, we present the invariant-mass distributions of the lepton pair for $B \to \pi \ell \nu_\ell$ ($\ell = \mu\,, \tau$) in the whole kinematic region. Finally, we discuss non-valence Fock state contributions to the $B \to \pi$ form factors $f_{B\pi}^{+}(q^2)$ and $f_{B\pi}^{0}(q^2)$ in brief.

* Corresponding author.
E-mail address: yuming.wang@tum.de (Y.-M. Wang).

http://dx.doi.org/10.1016/j.nuclphysb.2015.07.016

1. Introduction

Making every endeavor to achieve precision determinations of heavy-to-light transition form factors is of utmost importance to, on the one hand, test the CKM sector of the Standard Model, and on the other side to sharpen our knowledge towards diverse facets of the theory of strong interaction (QCD). We are continually surprised by complexities and subtleties of factorization properties and heavy quark expansions of even the simplest $B \to \pi$ form factors in the context of both QCD factorization and QCD sum rules on the light-cone (LCSR), not to mention more sophisticated $B \to \rho\,, K^*$ form factors with an unstable particle in the final states. The purposes of this paper are to pursue an endeavor to understand factorization structures of $B \to \pi$ form factors from the LCSR with B-meson distribution amplitudes (DAs) at $\mathcal{O}(\alpha_s)$ in QCD [1,2] (see also [3,4] for an alternative formulation in the framework of soft-collinear effective theory (SCET)); and to provide a complementary approach to anatomize the topical $|V_{ub}|$ tension arising from the mismatch in exclusive and inclusive determinations.

Constructions of the LCSR with B-meson DAs are accomplished by introducing the B-meson-to-vacuum correlation function, demonstrating factorization of the considered correlator in the proper kinematic regime, and applying the parton–hadron duality ansatz in the light-meson channel. It is evident that proof of QCD factorization for the correlation function defined with an on-shell B-meson state at next-to-leading order (NLO) constitutes a primary task in such program, in addition to further refinements of the duality relation. Inspecting the tree-level contribution to the correlation function shows that three different momentum modes with the scaling behaviors

$$\begin{aligned} P_\mu &\equiv (n\cdot P\,, \bar n\cdot P\,, P_\perp)\,, \qquad & P_{h\,,\,\mu} &\sim \mathcal{O}(1,1,1)\,, \\ P_{hc\,,\,\mu} &\sim \mathcal{O}(1,\lambda,\lambda^{1/2})\,, \qquad & P_{s\,,\,\mu} &\sim \mathcal{O}(\lambda,\lambda,\lambda)\,, \end{aligned} \tag{1}$$

appear in the problem under consideration, where n_μ and $\bar n_\mu$ are light-cone vectors, satisfying $n^2 = \bar n^2 = 0$ and $n\cdot\bar n = 2$, and are chosen such that the four-momentum of the fast-moving pion state has a large component $n\cdot p$ of order m_b. $P_{h\,,\,\mu}$, $P_{hc\,,\,\mu}$ and $P_{s\,,\,\mu}$ corresponding to the four-momentum of the external b-quark, of the interpolating current of pion and of the light-spectator quark, will be called hard, hard-collinear and soft modes hereafter. The transfer momentum q_μ of the weak current $\bar u\,\Gamma\, b$ can correspond to either a hard mode or a hard-collinear mode dependent on the kinematic region; a unified description for the purpose of demonstrating factorization of the correlation function at NLO can be achieved by focusing on the kinematic variable $n\cdot p$. The heavy-quark expansion parameter λ scales as Λ/m_b where Λ is a hadronic scale of order $\Lambda_{\rm QCD}$. It is well known that computing multi-scale amplitudes at loop level can be facilitated by applying the method of regions [5] in dimensional regularization, which has been extensively used for evaluating multi-loop integrals in heavy quarkonium decays, top-quark pair production near threshold, Higgs production at hadron colliders and last but not least B-meson decays. More importantly, we also benefit from a separation of dynamics at distinct energy scales allowing for resummation of large logarithms in the resulting matching coefficients and non-perturbative distribution functions with the standard renormalization-group (RG) approach in the momentum space. It is then our favored strategy to establish a factorization formula of the considered correlation function at leading power in Λ/m_b and at $\mathcal{O}(\alpha_s)$ using the method of regions.

The fundamental non-perturbative inputs entering LCSR discussed in this paper are the B-meson DAs defined by hadronic matrix elements of HQET string operators, which also serve as essential ingredients for the theoretical description of many other exclusive B-meson decays, e.g., the radiative leptonic $B \to \gamma\,\ell\,\nu_\ell$ decays. It will be shown that the constructed B-meson LCSR for $B \to \pi$ form factors are not only sensitive to the inverse moment of $\phi_B^+(\omega,\mu)$, i.e., $\lambda_B(\mu)$, but also dependent heavily on small ω behaviors of the B-meson DAs (see also [4]). We are therefore provided with a golden opportunity to probe more actuate images of the B meson in terms of the elementary constituents (quarks and gluons), anticipating precision measurements of differential q^2 distributions of $B \to \pi\,\ell\,\nu_l$ at high luminosity experiments and alternative (refined) determinations of $|V_{ub}|$ exclusively (for instance, the leptonic $B \to \tau\,\nu_\tau$ decay). We should also mention that understanding renormalization properties of the B-meson DAs and perturbative QCD constraints of $\phi_B^\pm(\omega,\mu)$ at high ω are also of conceptual interests for many reasons.

As diverse techniques for computing $B \to \pi$ form factors have been developed so far and theory predictions are continuously refined with yet higher precision, several comments on the state-of-art of QCD calculations might be meaningful.

- The up-to-date calculations of $B \to \pi$ form factors from the LCSR with pion DAs are restricted to NLO corrections to twist-2 and twist-3 terms [6–8] where asymptotic expressions of twist-3 DAs were taken to demonstrate factorization of the relevant correlation functions without bothering about mixing of the two- and three-particle DAs under renormalization. In addition, next-to-next-to-leading-order (NNLO) perturbative corrections to the twist-2 part induced by the running QCD coupling were fulfilled recently in [9]. Such computations should however be taken cum grano salis, because the large-β_0 approximation generally overestimates the complete perturbative corrections strongly. Further improvements of the pion LCSR, including complete NLO calculations of the twist-3 terms beyond the asymptotic limit and detailed analysis of the sub-leading power corrections from twist-5 and 6 parts, are highly desirable.
- The industries of investigating heavy-to-light B-meson form factors in QCD factorization were initiated in [10] where $\mathcal{O}(\alpha_s)$ corrections were found to be dominated by the spectator-scattering terms suffering sizeable uncertainty from $\lambda_B(\mu)$. Perturbative corrections to hard matching coefficients were carried out at one loop [11,12] for A-type currents and [12,13] for B-type currents, and at two loops [14–18] for A-type currents. The jet functions from integrating out dynamics of the hard-collinear fluctuation were accomplished at one-loop level [13,19,20]. One should however keep in mind that hadronic matrix elements of A-type currents (up to perturbatively calculable contributions dependent on the factorization schemes) cannot be further factorized in SCET(c, s) [21] and must be taken as fundamental inputs from other approaches.
- Yet another approach to compute $B \to \pi$ form factors is based upon transverse-momentum-dependent (TMD) QCD factorization for hard processes developed from the theory of on-shell Sudakov form factor [22] and the asymptotic behavior of elastic hadron–hadron scattering at high energy [23] with the underlying physical principle that the elastic scattering of an isolated parton suffers a strong suppression at high energy from radiative QCD corrections. Recently, computations of $B \to \pi$ form factors with TMD factorization approach have been pushed to $\mathcal{O}(\alpha_s)$ for twist-2 [24,25] and twist-3 [26] contributions of pion DAs. However, one needs to be aware of the fact that TMD factorization of hard exclusive processes becomes extraordinarily delicate due to complex infrared subtractions beyond the leading order in α_s [27] and a complete understanding of TMD factorization for exclusive

processes with large momentum transfer has not been achieved to date on the conceptual side.

The remainder of this paper is structured as follows. In Section 2 we briefly review the method of the LCSR with B-meson DAs by illustrating the tree-level calculation of $B \to \pi$ form factors. To facilitate proof of QCD factorization for the considered correlation function at NLO we recapitalize basic of the diagrammatical factorization approach at tree level as an instructive example. We then generalize factorization proof of the correction function to the one-loop order in Section 3 by showing a complete cancellation of soft contributions to the one-loop QCD diagrams and infrared subtractions determined by convolutions of the one-loop partonic DAs of the B-meson and the tree-level hard-scattering kernel, at leading power in Λ/m_b. Hard functions and jet functions entering factorization formulae of the correlation function are simultaneously obtained by computing the relevant one-loop integrals with the method of regions. Next-to-leading-logarithmic (NLL) resummation of the hard coefficient functions is performed by virtue of the RG approach and a detailed comparison of the obtained perturbative matching coefficients with the equivalent expressions computed in SCET is also presented in Section 3. We further derive NLL resummation improved LCSR for $B \to \pi$ form factors in Section 4, which constitute the main results of this paper. Phenomenological applications of the new sum rules are explored in Section 5, including determinations of the q^2 shapes of $B \to \pi$ form factors, extractions of the CKM matrix element $|V_{ub}|$ and predictions of the normalized q^2 distributions in $B \to \pi \ell \nu_\ell$. In Section 6 we turn to discuss the impact of three-particle B-meson DAs on $B \to \pi$ form factors, which is still the missing ingredient of our calculations. The concluding discussions are presented in Section 7. Appendix A contains some useful expressions of one-loop integrals after expanding integrands with the method of regions. Spectral representations of the convolution integrals for constructing the LCSR with B-meson DAs and two-point QCD sum rules for the decay constants of the B-meson and the pion are collected in Appendices B and C.

2. Recapitulation of the LCSR method

We construct LCSR of the form factors $f_{B\pi}^+(q^2)$ and $f_{B\pi}^0(q^2)$ with the correlation function

$$\begin{aligned}\Pi_\mu(n\cdot p, \bar n\cdot p) &= \int d^4x\, e^{ip\cdot x}\langle 0|T\left\{\bar d(x)\not{\bar n}\gamma_5 u(x), \bar u(0)\gamma_\mu b(0)\right\}|\bar B(p+q)\rangle \\ &= \Pi(n\cdot p, \bar n\cdot p)\, n_\mu + \widetilde\Pi(n\cdot p, \bar n\cdot p)\,\bar n_\mu\,, \end{aligned} \tag{2}$$

defined with a pion interpolating current carrying a four-momentum p_μ and a weak $b \to u$ transition current. We work in the rest frame of the B-meson with the velocity vector satisfying $n\cdot v = \bar n\cdot v = 1$ and $v_\perp = 0$. For definiteness, we adopt the following conventions

$$n\cdot p \simeq \frac{m_B^2 + m_\pi^2 - q^2}{m_B} = 2E_\pi\,, \qquad \bar n\cdot p \sim \mathcal{O}(\Lambda_{\rm QCD})\,. \tag{3}$$

The correlation function $\Pi_\mu(n\cdot p, \bar n\cdot p)$ can be computed from light-cone operator–product–expansion (OPE) at $\bar n\cdot p < 0$. Evaluating the diagram in Fig. 1 yields

$$\begin{aligned}\widetilde\Pi(n\cdot p, \bar n\cdot p) &= \tilde f_B(\mu)\, m_B \int_0^\infty d\omega'\, \frac{\phi_B^-(\omega')}{\omega' - \bar n\cdot p - i\,0} + \mathcal{O}(\alpha_s)\,, \\ \Pi(n\cdot p, \bar n\cdot p) &= \mathcal{O}(\alpha_s)\,. \end{aligned} \tag{4}$$

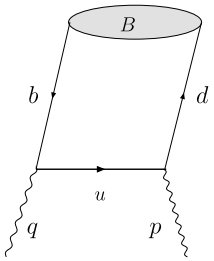

Fig. 1. Diagrammatical representation of the correlation function $\Pi_\mu(n\cdot p, \bar n\cdot p)$ at tree level.

The B-meson distribution amplitude (DA) $\phi_B^-(\omega')$ is defined as [28]

$$\begin{aligned}&\langle 0|\bar d_\beta(\tau\bar n)\,[\tau\bar n,0]\,b_\alpha(0)|\bar B(p+q)\rangle\\&\quad=-\frac{i\,\tilde f_B(\mu)\,m_B}{4}\left\{\frac{1+\not v}{2}\left[2\tilde\phi_B^+(\tau)+\left(\tilde\phi_B^-(\tau)-\tilde\phi_B^+(\tau)\right)\not n\right]\gamma_5\right\}_{\alpha\beta},\end{aligned}\tag{5}$$

where the light-cone Wilson line is given by

$$[\tau\bar n,0]=\mathrm{P}\left\{\mathrm{Exp}\left[i\,g_s\int_0^\tau d\lambda\,\bar n\cdot A(\lambda\bar n)\right]\right\},\tag{6}$$

with the convention of the covariant derivative in QCD as $D_\mu=\partial_\mu-i\,g_s\,T^a\,A_\mu^a$, and the Fourier transformations of $\tilde\phi_B^\pm(\tau)$ lead to

$$\phi_B^\pm(\omega')=\int_{-\infty}^{+\infty}\frac{d\,\tau}{2\,\pi}\,e^{i\,\omega'\,\tau}\,\tilde\phi_B^\pm(\tau-i0)\,.\tag{7}$$

One then can construct the light-cone projector in momentum space [4]

$$\begin{aligned}M_{\beta\alpha}=&-\frac{i\,\tilde f_B(\mu)\,m_B}{4}\\&\times\left\{\frac{1+\not v}{2}\left[\phi_B^+(\omega')\not n+\phi_B^-(\omega')\not{\bar n}-\frac{2\,\omega'}{D-2}\,\phi_B^-(\omega')\,\gamma_\perp^\rho\,\frac{\partial}{\partial k'_{\perp\rho}}\right]\gamma_5\right\}_{\alpha\beta}\end{aligned}\tag{8}$$

in D dimensions. Here, $\tilde f_B(\mu)$ is the B-meson decay constant in the static limit and it can be expressed in terms of the QCD decay constant

$$f_B=\tilde f_B(\mu)\left[1+\frac{\alpha_s\,C_F}{4\,\pi}\left(-3\,\ln\frac{\mu}{m_b}-2\right)\right].\tag{9}$$

Note that a single B-meson DA $\phi_B^-(\omega')$ appears in the tree-level LCSR (4) in contrast to factorization of $B\to\gamma\,\ell\,\nu$ where only $\phi_B^+(\omega')$ enters the factorization formulae of the form factors $F_{V,A}\,(E_\gamma)$ at leading power in Λ/m_b [29]. The discrepancy can be traced back to the longitudinally polarized interpolating current for the pion in the former and to the transversely polarized photon in the latter.

Factorization of $\Pi_\mu(n\cdot p,\bar n\cdot p)$ at tree level is straightforward due to the absence of infrared (soft) divergences. The hard-collinear fluctuation of the internal u-quark guarantees light-cone

expansion of the non-local matrix element defining the B-meson DAs. For the sake of a clear demonstration of factorization of $\Pi_\mu(n\cdot p, \bar n\cdot p)$ at one-loop order, we write down the tree-level approximation of the partonic correlation function[1] (defined as replacing $|\bar B(p+q)\rangle$ by $|b(p_B-k)\bar d(k)\rangle$ in Eq. (2) with $p_B\equiv p+q$)

$$\Pi^{(0)}_{\mu,b\bar d}(n\cdot p,\bar n\cdot p)=\int d\omega'\, T^{(0)}_{\alpha\beta}(n\cdot p,\bar n\cdot p,\omega')\Phi^{(0)\,\alpha\beta}_{b\bar d}(\omega')\,, \tag{10}$$

where the superscript (0) indicates the tree level, the Lorenz index "μ" is suppressed on the right-hand side, the leading-order hard-scattering kernel is given by

$$T^{(0)}_{\alpha\beta}(n\cdot p,\bar n\cdot p,\omega')=\frac{i}{2}\,\frac{1}{\bar n\cdot p-\omega'+i0}\left[\not n\gamma_5\not{\bar n}\gamma_\mu\right]_{\alpha\beta}\,, \tag{11}$$

and the partonic DA of the B-meson reads

$$\Phi^{\alpha\beta}_{b\bar d}(\omega')=\int\frac{d\tau}{2\pi}\,e^{i\,\omega'\,\tau}\langle 0|\bar d_\beta(\tau\,\bar n)\,[\tau\bar n,0]\,b_\alpha(0)|b(p_B-k)\bar d(k)\rangle \tag{12}$$

with the tree-level contribution

$$\Phi^{(0)\,\alpha\beta}_{b\bar d}(\omega')=\delta(\bar n\cdot k-\omega')\,\bar d_\beta(k)\;b_\alpha(p_B-k)\,. \tag{13}$$

It is worthwhile to point out that the variable ω' is not necessarily to be the same as $\omega\equiv\bar n\cdot k$ despite the equivalence at tree level. The partonic light-cone projector can be obtained from Eq. (8) via the replacement $\phi^\pm_B(\omega')\to\phi^\pm_{b\bar d}(\omega')$, and we can write down

$$\begin{aligned}&\Pi^{(0)}_{\mu\,,b\bar d}(n\cdot p,\bar n\cdot p)=\Pi^{(0)}_{b\bar d}(n\cdot p,\bar n\cdot p)\,n_\mu+\widetilde\Pi^{(0)}_{b\bar d}(n\cdot p,\bar n\cdot p)\,\bar n_\mu\,,\\&\widetilde\Pi^{(0)}_{b\bar d}(n\cdot p,\bar n\cdot p)=\tilde f_B(\mu)\,m_B\,\frac{\phi^-_{b\bar d}(\omega)}{\omega-\bar n\cdot p-i\,0}\,,\qquad\Pi^{(0)}_{b\bar d}(n\cdot p,\bar n\cdot p)=0\,.\end{aligned} \tag{14}$$

With definitions of the $B\to\pi$ form factors and the pion decay constant

$$\begin{aligned}&\langle\pi(p)|\bar u\gamma_\mu b|\bar B(p_B)\rangle=f^+_{B\pi}(q^2)\left[p_B+p-\frac{m_B^2-m_\pi^2}{q^2}q\right]_\mu+f^0_{B\pi}(q^2)\,\frac{m_B^2-m_\pi^2}{q^2}q_\mu\,,\\&\langle\pi(p)|\bar d\not n\gamma_5 u|0\rangle=-i\,n\cdot p\,f_\pi\,,\end{aligned} \tag{15}$$

we obtain the hadronic dispersion relation for the correlation function

$$\begin{aligned}&\Pi_\mu(n\cdot p,\bar n\cdot p)\\&\quad=\frac{f_\pi\,n\cdot p\,m_B}{2\,(m_\pi^2-p^2)}\left\{\bar n_\mu\left[\frac{n\cdot p}{m_B}\,f^+_{B\pi}(q^2)+f^0_{B\pi}(q^2)\right]\right.\\&\qquad\left.+\,n_\mu\,\frac{m_B}{n\cdot p-m_B}\left[\frac{n\cdot p}{m_B}\,f^+_{B\pi}(q^2)-f^0_{B\pi}(q^2)\right]\right\}\\&\qquad+\int\limits_{\omega_s}^{+\infty}d\omega'\,\frac{1}{\omega'-\bar n\cdot p-i0}\left[\rho^h(\omega',n\cdot p)\,n_\mu+\tilde\rho^h(\omega',n\cdot p)\,\bar n_\mu\right],\end{aligned} \tag{16}$$

[1] Perturbative matching coefficients entering the factorization formulae of $\Pi_\mu(n\cdot p,\bar n\cdot p)$ are independent of the external partonic state, and it is a matter of convenience to choose a certain configuration for the practical calculation. More detailed discussions of this point in the context of factorization of $B\to\gamma\ell\nu$ can be found in Ref. [30].

where ω_s is the hadronic threshold in the pion channel. Applying the quark–hadron duality ansatz, the integrals over the hadronic spectral densities can be approximated by the integrals over the QCD spectral functions with the threshold parameter reinterpreted as an effective "internal" parameter of the sum rule approach. Then, one can derive the final expressions of the LCSR after implementing the Borel transformation in the variable $\bar{n}\cdot p \to \omega_M$

$$f_{B\pi}^{+}(q^2) = \frac{\tilde{f}_B(\mu)\, m_B}{f_\pi\, n\cdot p} \exp\left[\frac{m_\pi^2}{n\cdot p\;\omega_M}\right] \int_0^{\omega_s} d\omega'\, e^{-\omega'/\omega_M}\, \phi_B^{-}(\omega') + \mathcal{O}(\alpha_s)\,,$$
$$f_{B\pi}^{0}(q^2) = \frac{n\cdot p}{m_B}\, f_{B\pi}^{+}(q^2) + \mathcal{O}(\alpha_s)\,, \tag{17}$$

which are in agreement with Refs. [2,3].

Albeit with the rather simple structures of the tree-level LCSR, some interesting observations can be already made.

- Since the B-meson DA $\phi_B^{+}(\omega')$ does not enter the factorization formulae of $\Pi_\mu(n\cdot p, \bar{n}\cdot p)$ at tree level and $\phi_B^{\pm}(\omega')$ do not mix under renormalization at one loop in the massless light-quark limit, the convolution integrals of $\phi_B^{+}(\omega')$ entering the contributions of the one-loop diagrams of $\Pi_\mu(n\cdot p, \bar{n}\cdot p)$ in QCD must be infrared finite at $\mathcal{O}(\alpha_s)$ to guarantee the validity of QCD factorization of $\Pi_\mu(n\cdot p, \bar{n}\cdot p)$.
- Since only a single invariant function $\widetilde{\Pi}(n\cdot p, \bar{n}\cdot p)$ survives at tree level, one concludes that the one-loop contributions to $\Pi(n\cdot p, \bar{n}\cdot p)$ in QCD must be infrared finite due to the vanishing infrared (soft) subtraction at $\mathcal{O}(\alpha_s)$, provided that factorization of $\Pi_\mu(n\cdot p, \bar{n}\cdot p)$ holds.
- The Borel mass ω_M and the threshold parameter ω_s enter into the LCSR from the dispersive analysis with respect to the variable $\bar{n}\cdot p$, indicating that one needs to identify $\omega_M = M^2/n\cdot p$ and $\omega_s = s_0/n\cdot p$ with (M^2, s_0) from the dispersive construction of the LCSR in the variable p^2. From the scaling $M^2 \sim s_0 \sim \Lambda^2$, one then finds the power counting of $f_{B\pi}^{+}$ and $f_{B\pi}^{0}$ as $\sim (\Lambda/m_b)^{3/2}$ at tree level, consistent with the observations of [10,21].

3. Factorization of the correlation function at $\mathcal{O}(\alpha_s)$

The objective of this section is to establish the factorization formulae for $\Pi_\mu(n\cdot p, \bar{n}\cdot p)$ in QCD at one-loop level. We adopt the diagrammatic factorization method expanding the correlator $\Pi_{\mu,\, b\bar{d}}$, the short-distance function T and the partonic DA of the B meson $\Phi_{b\bar{d}}$ in perturbation theory. Schematically,

$$\begin{aligned}\Pi_{\mu,\, b\bar{d}} &= \Pi_{\mu,\, b\bar{d}}^{(0)} + \Pi_{\mu,\, b\bar{d}}^{(1)} + \ldots = \Phi_{b\bar{d}} \otimes T \\ &= \Phi_{b\bar{d}}^{(0)} \otimes T^{(0)} + \left[\Phi_{b\bar{d}}^{(0)} \otimes T^{(1)} + \Phi_{b\bar{d}}^{(1)} \otimes T^{(0)}\right] + \ldots\,,\end{aligned} \tag{18}$$

where $\otimes$ denotes the convolution in the variable ω' defined in Eq. (12), and the superscripts indicate the order of α_s. The hard-scattering kernel at $\mathcal{O}(\alpha_s)$ is then determined by the matching condition

$$\Phi_{b\bar{d}}^{(0)} \otimes T^{(1)} = \Pi_{\mu,\, b\bar{d}}^{(1)} - \Phi_{b\bar{d}}^{(1)} \otimes T^{(0)}\,, \tag{19}$$

where the second term serves as the infrared (soft) subtraction. One crucial point in the proof of factorization of $\Pi_{\mu,\, b\bar{d}}$ is to demonstrate that the hard-scattering kernel T can be contributed only

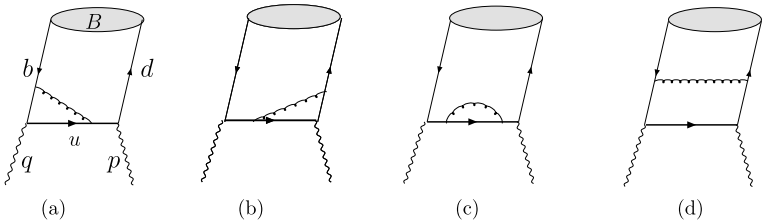

Fig. 2. Diagrammatical representation of the correlation function $\Pi_\mu(n\cdot p, \bar{n}\cdot p)$ at $\mathcal{O}(\alpha_s)$.

from hard and/or hard-collinear regions at leading power in Λ/m_b, due to a complete cancellation of the soft contribution to $\Pi^{(1)}_{\mu,\,b\bar{d}}$ and $\Phi^{(1)}_{b\bar{d}}\otimes T^{(0)}$. In addition, since B-meson DAs can only collect the soft QCD dynamics of $\Pi_{\mu,\,b\bar{d}}$, we must show that there is no leading contribution to the correlation function from the collinear region (with the momentum scaling $l_\mu\sim(1,\lambda^2,\lambda)$) at leading power.

Following Ref. [30], we will evaluate the master formula of $T^{(1)}$ in Eq. (19) diagram by diagram. However, we will apply the method of regions [5] to compute the loop integrals in order to obtain the hard coefficient function (C) and the jet function (J) simultaneously. To establish the factorization formula

$$\Pi_{\mu,\,b\bar{d}}=\Phi_{b\bar{d}}\otimes T=C\cdot J\otimes\Phi_{b\bar{d}}\,, \tag{20}$$

C and J must be well defined in dimensional regularization. This guarantees that we can adopt dimensional regularization to evaluate the leading-power contributions of $\Pi_{\mu,\,b\bar{d}}$ without introducing an additional "analytical" regulator. The strategies of our calculations are as follows: (i) Identify leading regions of the scalar integral for each diagram; (ii) Simplify the Dirac algebra in the numerator for a given leading region and evaluate the relevant integrals using the method of regions; (iii) Evaluate the hard and hard-collinear contributions with the light-cone projector of the B meson in momentum space; (iv) Show the equivalence of the soft subtraction term and the correlation function in the soft region; (v) Add up the contributions from the hard and hard-collinear regions separately.

3.1. Weak vertex diagram

The contribution to $\Pi^{(1)}_\mu$ from the QCD correction to the weak vertex (the diagram in Fig. 2(a)) is

$$\begin{aligned}\Pi^{(1)}_{\mu,\,weak}=&\frac{g_s^2\,C_F}{2\,(\bar{n}\cdot p-\omega)}\int\frac{d^Dl}{(2\pi)^D}\,\frac{1}{[(p-k+l)^2+i0][(m_b v+l)^2-m_b^2+i0][l^2+i0]}\\&\times\bar{d}(k)\not{n}\,\gamma_5\not{\bar{n}}\,\gamma_\rho\,(\not{p}-\not{k}+\not{l})\,\gamma_\mu\,(m_b\not{v}+\not{l}+m_b)\,\gamma^\rho\,b(v)\,,\end{aligned} \tag{21}$$

where the label "$b\bar{d}$" of the partonic correlation function $\Pi_{\mu,\,b\bar{d}}$ will be suppressed from now on and $D=4-2\epsilon$. Since the perturbative matching coefficients are insensitive to infrared physics, we thus assign the external momenta $m_b\,v$ to the bottom quark and k (with $k^2=0$) to the light quark. In accordance with the scaling behaviors

$$n\cdot p\sim m_b\,,\qquad \bar{n}\cdot p\sim\Lambda\,,\qquad k_\mu\sim\Lambda\,, \tag{22}$$

we identify the leading-power contributions of the scalar integral

$$I_1 = \int [d\,l]\,\frac{1}{[(p-k+l)^2+i0][(m_b v+l)^2-m_b^2+i0][l^2+i0]} \tag{23}$$

from the hard, hard-collinear and soft regions and the power counting $I_1 \sim \lambda^0$ implies that only the leading-power contributions of the numerator in Eq. (21) need to be kept for a given region taking into account the power counting of the tree-level contribution in Eq. (11). We define the integration measure as

$$[d\,l] \equiv \frac{(4\pi)^2}{i}\left(\frac{\mu^2 e^{\gamma_E}}{4\pi}\right)^{\epsilon}\frac{d^D l}{(2\pi)^D}\,. \tag{24}$$

Inserting the partonic light-cone projector yields the hard contribution of $\Pi^{(1)}_{\mu,weak}$ at leading power

$$\begin{aligned}\Pi^{(1),\,h}_{\mu,\,weak} = {} & i\,g_s^2\,C_F\,\tilde{f}_B(\mu)\,m_B\,\frac{\phi^-_{b\bar{d}}(\omega)}{\bar{n}\cdot p-\omega}\int\frac{d^D l}{(2\pi)^D} \\ & \frac{1}{[l^2+n\cdot p\,\bar{n}\cdot l+i0][l^2+2\,m_b\,v\cdot l+i0][l^2+i0]} \\ & \times\left\{\bar{n}_\mu\left[2\,m_b\,n\cdot(p+l)+(D-2)\,l_\perp^2\right]-n_\mu\,(D-2)\,(\bar{n}\cdot l)^2\right\},\end{aligned} \tag{25}$$

where the superscript "h" denotes the hard contribution and we adopt the conventions

$$l_\perp^2 \equiv g_\perp^{\mu\nu}\,l_\mu\,l_\nu\,, \qquad g_\perp^{\mu\nu} \equiv g^{\mu\nu}-\frac{n^\mu\bar{n}^\nu}{2}-\frac{n^\nu\bar{n}^\mu}{2}\,. \tag{26}$$

Using the results of loop integrals provided in Appendix A, we obtain

$$\begin{aligned}\Pi^{(1),\,h}_{\mu,\,weak} = {} & \frac{\alpha_s\,C_F}{4\pi}\,\tilde{f}_B(\mu)\,m_B\,\frac{\phi^-_{b\bar{d}}(\omega)}{\bar{n}\cdot p-\omega}\left\{\bar{n}_\mu\left[\frac{1}{\epsilon^2}+\frac{1}{\epsilon}\left(2\ln\frac{\mu}{n\cdot p}+1\right)+2\ln^2\frac{\mu}{n\cdot p}\right.\right. \\ & \left.+2\ln\frac{\mu}{m_b}-\ln^2 r-2\,\mathrm{Li}_2\left(-\frac{\bar{r}}{r}\right)+\frac{2-r}{r-1}\ln r+\frac{\pi^2}{12}+3\right] \\ & \left.+n_\mu\left[\frac{1}{r-1}\left(1+\frac{r}{\bar{r}}\ln r\right)\right]\right\},\end{aligned} \tag{27}$$

with $r = n\cdot p/m_b$ and $\bar{r} = 1-r$.

Along the same vein, one can identify the hard-collinear contribution of $\Pi^{(1)}_{\mu,\,weak}$ at leading power

$$\begin{aligned}\Pi^{(1),\,hc}_{\mu,\,weak} = {} & i\,g_s^2\,C_F\,\tilde{f}_B(\mu)\,m_B\,\frac{\phi^-_{b\bar{d}}(\omega)}{\bar{n}\cdot p-\omega}\int\frac{d^D l}{(2\pi)^D} \\ & \frac{2\,m_b\,n\cdot(p+l)}{[n\cdot(p+l)\,\bar{n}\cdot(p-k+l)+l_\perp^2+i0][m_b\,n\cdot l+i0][l^2+i0]}\,,\end{aligned} \tag{28}$$

where the superscript "hc" indicates the hard-collinear contribution and the propagators have been expanded systematically in the hard-collinear region. Evaluating the integrals with the relations collected in Appendix A yields

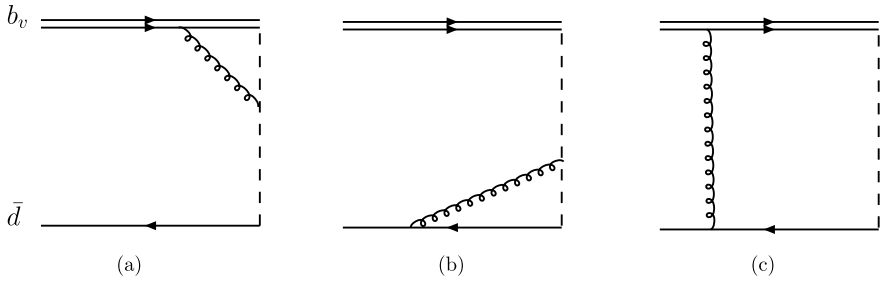

Fig. 3. One-loop diagrams for the B-meson DA $\Phi^{\alpha\beta}_{b\bar{u}}(\omega')$ defined in (12).

$$\Pi^{(1),\,hc}_{\mu,\,weak} = \frac{\alpha_s\,C_F}{4\pi}\,\tilde{f}_B(\mu)\,m_B\,\frac{\phi^{-}_{b\bar{d}}(\omega)}{\omega-\bar{n}\cdot p}\,\bar{n}_\mu\left[\frac{2}{\epsilon^2}+\frac{2}{\epsilon}\left(\ln\frac{\mu^2}{n\cdot p\,(\omega-\bar{n}\cdot p)}+1\right)\right.$$
$$\left.+\ln^2\frac{\mu^2}{n\cdot p\,(\omega-\bar{n}\cdot p)}+2\ln\frac{\mu^2}{n\cdot p\,(\omega-\bar{n}\cdot p)}-\frac{\pi^2}{6}+4\right]. \tag{29}$$

Applying the method of regions we extract the soft contribution of $\Pi^{(1)}_{\mu,weak}$

$$\Pi^{(1),\,s}_{\mu,\,weak} = \frac{g_s^2\,C_F}{2\,(\bar{n}\cdot p-\omega)}\int\frac{d^D l}{(2\pi)^D}\,\frac{1}{[\bar{n}\cdot(p-k+l)+i0][v\cdot l+i0][l^2+i0]}$$
$$\bar{d}(k)\,\not{n}\,\gamma_5\,\bar{\not{n}}\,\gamma_\mu\,b(p_b)$$
$$=\frac{\alpha_s\,C_F}{4\pi}\,\tilde{f}_B(\mu)\,m_B\,\frac{\phi^{-}_{b\bar{d}}(\omega)}{\bar{n}\cdot p-\omega}\,\bar{n}_\mu$$
$$\times\left[\frac{1}{\epsilon^2}+\frac{2}{\epsilon}\ln\frac{\mu}{\omega-\bar{n}\cdot p}+2\ln^2\frac{\mu}{\omega-\bar{n}\cdot p}+\frac{3\pi^2}{4}\right], \tag{30}$$

where the superscript "s" represents the soft contribution.

Now, we compute the corresponding infrared subtraction term $\Phi^{(1)}_{b\bar{d},\,a}\otimes T^{(0)}$ as displayed in Fig. 3(a). With the Wilson-line Feynman rules, we obtain

$$\Phi^{\alpha\beta\,,(1)}_{b\bar{d},\,a}(\omega,\omega') = i\,g_s^2\,C_F\int\frac{d^D l}{(2\pi)^D}\,\frac{1}{[\bar{n}\cdot l+i0][v\cdot l+i0][l^2+i0]}$$
$$\times\,[\delta(\omega'-\omega-\bar{n}\cdot l)-\delta(\omega'-\omega)]\,[\bar{d}(k)]_\alpha\,[b(v)]_\beta\ , \tag{31}$$

from which we can derive the soft subtraction term

$$\Phi^{(1)}_{b\bar{d},\,a}\otimes T^{(0)} = \frac{g_s^2\,C_F}{2\,(\bar{n}\cdot p-\omega)}\int\frac{d^D l}{(2\pi)^D}\,\frac{1}{[\bar{n}\cdot(p-k+l)+i0][v\cdot l+i0][l^2+i0]}$$
$$\bar{d}(k)\,\not{n}\,\gamma_5\,\bar{\not{n}}\,\gamma_\mu\,b(v)\ , \tag{32}$$

where the tree-level hard kernel in Eq. (11) is used. We then conclude that

$$\Pi^{(1),\,s}_{\mu,\,weak} = \Phi^{(1)}_{b\bar{d},\,a}\otimes T^{(0)} \tag{33}$$

at leading power in Λ/m_b, which is an essential point to prove factorization of the correlation function Π_μ.

3.2. Pion vertex diagram

Now we turn to compute the QCD correction to the pion vertex (the diagram in Fig. 2b)

$$\Pi^{(1)}_{\mu,\,pion} = -\frac{g_s^2\,C_F}{n\cdot p\,(\bar n\cdot p-\omega)}\int\frac{d^D l}{(2\pi)^D}\,\frac{1}{[(p-l)^2+i0][(l-k)^2+i0][l^2+i0]} \bar d(k)\,\gamma_\rho\,\not{l}\not{n}\,\gamma_5\,(\not{p}-\not{l})\,\gamma^\rho\,(\not{p}-\not{k})\,\gamma_\mu\,b(v)\,. \tag{34}$$

One can identify the leading-power contributions of the scalar integral

$$I_2 = \int[d\,l]\,\frac{1}{[(p-l)^2+i0][(l-k)^2+i0][l^2+i0]} \tag{35}$$

from the hard-collinear and soft regions, which have the scaling behaviors

$$I_2^{hc}\sim I_2^{s}\sim\lambda^{-1}\,, \tag{36}$$

by virtue of the power counting analysis. It is evident that the pion vertex correction would give rise to the power enhanced effect in relative to the tree-level contribution of Eq. (11), provided that no additional suppression factors come from the spinor structure. Closer inspection shows that expanding the integrand of I_2 in the soft region will generate a scaleless integral which vanishes in dimensional regularization. For the hard-collinear loop momentum, the spinor structure is reduced to

$$\bar d(k)\,[...]\,b(v) = \bar d(k)\,\gamma_5\,[2\,(\not{p}-\not{l})\,\not{n}\,\not{l}+(D-4)\,\not{l}\not{n}\,(\not{p}-\not{l})]\,(\not{p}-\not{k})\,b(v) \tag{37}$$

which indeed induces a power-suppression factor λ. It turns out to be less transparent to extract the leading-power contribution in the hard-collinear region with the insertion of the B-meson light-cone projector. Instead, we first compute the loop integral of Eq. (34) exactly without resorting to the method of regions; then we express $\Pi^{(1)}_{\mu,\,pion}$ in terms of the partonic DAs by inserting the momentum-space projector.

Employing the expressions of loop integrals in Appendix A we find

$$\begin{aligned}\Pi^{(1)}_{\mu,\,pion} = \Pi^{(1),\,hc}_{\mu,\,pion} = \frac{\alpha_s\,C_F}{4\pi}\,\tilde f_B(\mu)\,m_B\,\frac{1}{\bar n\cdot p-\omega}\,\Bigg\{ & n_\mu\,\phi^+_{b\bar d}(\omega)\left[\frac{\bar n\cdot p-\omega}{\omega}\,\ln\frac{\bar n\cdot p-\omega}{\bar n\cdot p}\right] \\ & +\bar n_\mu\,\phi^-_{b\bar d}(\omega)\left[\left(\frac{1}{\epsilon}+\ln\left(-\frac{\mu^2}{p^2}\right)\right)\left(\frac{2\,\bar n\cdot p}{\omega}\,\ln\frac{\bar n\cdot p-\omega}{\bar n\cdot p}+1\right)\right. \\ & \left.-\frac{\bar n\cdot p}{\omega}\,\ln\frac{\bar n\cdot p-\omega}{\bar n\cdot p}\left(\ln\frac{\bar n\cdot p-\omega}{\bar n\cdot p}+\frac{2\omega}{\bar n\cdot p}-4\right)+4\right]\Bigg\}\,.\end{aligned} \tag{38}$$

While the soft contribution of $\Pi^{(1)}_{\mu,\,pion}$ vanishes in dimensional regularization, it remains to demonstrate that the precise cancellation of $\Pi^{(1),\,s}_{\mu,\,pion}$ and $\Phi_{b\bar d,\,b}\otimes T^{(0)}$ is independent of regularization schemes. Applying the method of regions yields

$$\Pi^{(1),\,s}_{\mu,\,pion} = -\frac{g_s^2\,C_F}{2\,(\bar n\cdot p-\omega)}\int\frac{d^D l}{(2\pi)^D}\,\frac{1}{[\bar n\cdot(p-l)+i0][(l-k)^2+i0][l^2+i0]} \bar d(k)\,\not{\bar n}\,\not{l}\not{n}\,\gamma_5\,\not{\bar n}\,\gamma_\mu\,b(v)\,. \tag{39}$$

The corresponding contribution to the partonic DA (the diagram in Fig. 3b) is given by

$$\Phi^{\alpha\beta,(1)}_{b\bar{d},\,b}(\omega,\omega') = ig_s^2\,C_F\int\frac{d^Dl}{(2\pi)^D}\,\frac{1}{[\bar{n}\cdot l+i0][(k+l)+i0][l^2+i0]} \times[\delta(\omega'-\omega-\bar{n}\cdot l)-\delta(\omega'-\omega)]\,[\bar{d}(k)\,\bar{n}\!\!\!/\,(k\!\!\!/+l\!\!\!/)]_\alpha\,[b(v)]_\beta\,. \tag{40}$$

One then deduces the soft subtraction term

$$\Phi^{(1)}_{b\bar{d},\,b}\otimes T^{(0)} = -\frac{g_s^2\,C_F}{2\,(\bar{n}\cdot p-\omega)}\int\frac{d^Dl}{(2\pi)^D}\,\frac{1}{[\bar{n}\cdot(p-k-l)+i0][(k+l)^2+i0][l^2+i0]} \bar{d}(k)\,\bar{n}\!\!\!/\,(k\!\!\!/+l\!\!\!/)\,n\!\!\!/\,\gamma_5\,\bar{n}\!\!\!/\,\gamma_\mu\,b(v)\,, \tag{41}$$

which coincides with $\Pi^{(1),\,s}_{\mu,\,pion}$ exactly after the shift of the loop momentum $l\to l-k$.

3.3. Wave function renormalization

The self-energy correction to the intermediate quark propagator (the diagram in Fig. 2c) can be written as

$$\Pi^{(1)}_{\mu,\,wfc} = \frac{g_s^2\,C_F}{(n\cdot p)^2\,(\bar{n}\cdot p-\omega)^2}\int\frac{d^Dl}{(2\pi)^D}\,\frac{1}{[(p-k+l)^2+i0][l^2+i0]} \bar{d}(k)n\!\!\!/\,\gamma_5\,(p\!\!\!/-k\!\!\!/)\,\gamma_\rho\,(p\!\!\!/-k\!\!\!/+l\!\!\!/)\,\gamma^\rho\,(p\!\!\!/-k\!\!\!/)\,\gamma_\mu\,b(v)\,. \tag{42}$$

Apparently, $\Pi^{(1)}_{\mu,\,wfc}$ is free of soft and collinear divergences and a straightforward calculation gives

$$\Pi^{(1)}_{\mu,\,wfc} = \frac{\alpha_s\,C_F}{4\pi}\,\tilde{f}_B(\mu)\,m_B\,\frac{\phi^-_{b\bar{d}}(\omega)}{\bar{n}\cdot p-\omega}\,\bar{n}_\mu\left[\frac{1}{\epsilon}+\ln\frac{\mu^2}{n\cdot p\,(\omega-\bar{n}\cdot p)}+1\right]. \tag{43}$$

Now we evaluate the perturbative matching coefficient from the wave function renormalization of the external quark fields. It is evident that the wave function renormalization of a massless quark does not contribute to the matching coefficient when dimensional regularization is applied to regularize both ultraviolet and infrared divergences, i.e.,

$$\Pi^{(1)}_{\mu,\,dwf} - \Phi^{(1)}_{b\bar{d},\,dwf}\otimes T^{(0)} = 0\,. \tag{44}$$

The wave function renormalization of the b-quark in QCD gives

$$\Pi^{(1)}_{\mu,\,bwf} = -\frac{\alpha_s\,C_F}{8\pi}\left[\frac{3}{\epsilon}+3\,\ln\frac{\mu^2}{m_b^2}+4\right]\Pi^{(0)}_\mu\,, \tag{45}$$

with $\Pi^{(0)}_\mu$ displayed in Eq. (14). The wave function renormalization of the b-quark in HQET is

$$\Phi^{(1)}_{b\bar{d},\,bwf}\otimes T^{(0)} = 0\,, \tag{46}$$

due to the scaleless integral, we then find

$$\Pi^{(1)}_{\mu,\,bwf} - \Phi^{(1)}_{b\bar{d},\,bwf}\otimes T^{(0)} = -\frac{\alpha_s\,C_F}{8\pi}\left[\frac{3}{\epsilon}+3\,\ln\frac{\mu^2}{m_b^2}+4\right]\Pi^{(0)}_\mu\,. \tag{47}$$

3.4. Box diagram

The one-loop contribution to Π_μ from the box diagram is given by

$$\Pi^{(1)}_{\mu,\,box} = g_s^2\, C_F \int \frac{d^D l}{(2\pi)^D} \frac{-1}{[(m_b v + l)^2 - m_b^2 + i0][(p-k+l)^2 + i0][(k-l)^2 + i0][l^2 + i0]} \bar{d}(k)\, \gamma_\rho\, (\not{k} - \not{l}) \not{n}\, \gamma_5\, (\not{p} - \not{k} + \not{l})\, \gamma_\mu\, (m_b \not{v} + \not{l} + m_b)\, \gamma^\rho\, b(v)\,. \tag{48}$$

This is the only diagram at one-loop level without a hard-collinear propagator outside of the loop, hence we must identify the enhancement factor m_b/Λ from the corresponding scalar integral so that it can give rise to the leading-power contribution compared to the tree-level amplitude in Eq. (14). With the scaling behaviors of the external momenta, one can establish the scaling of

$$I_4 = \int [d\,l] \frac{1}{[(m_b v + l)^2 - m_b^2 + i0][(p-k+l)^2 + i0][(k-l)^2 + i0][l^2 + i0]} \tag{49}$$

as λ^{-1} (λ^{-2}) in the hard-collinear and semi-hard (soft) regions.[2] It is straightforward to verify that the semi-hard contribution will be reduced to a scaleless integral, since there is no external semi-hard mode in the box diagram. We are only left with the hard-collinear and soft regions at leading power in Λ/m_b. The term $(\not{k} - \not{l})$ in the spinor structure will give a suppression factor λ in the soft region so that both the hard-collinear and the soft contributions are of the same power. One might be curious about the observation that the box diagram contributes to the jet function entering the factorization formulae of the B-meson-to-vacuum correlation function Π_μ at one-loop level while the hard-collinear contribution of the box diagram vanishes in the radiative leptonic decay $B \to \gamma \ell \nu$ [30,31]. The crucial discrepancy attributes to the longitudinally polarized pion interpolating current in the former and the transversely polarized photon in the latter. As a consequence, one is not able to pick up the large components of two intermediate up-quark propagators

$$(\not{k} - \not{l})\, \not{\epsilon}^*_\gamma\, (\not{p} - \not{k} + \not{l}) \tag{50}$$

simultaneously in the case of $B \to \gamma \ell \nu$, while this is possible in the contribution of the box diagram for Π_μ as indicated in Eq. (48).

Evaluating the hard-collinear contribution of $\Pi^{(1)}_{\mu,\,box}$ with the partonic momentum-space projector yields

$$\Pi^{(1),\,hc}_{\mu,\,box} = i\, g_s^2\, C_F\, \tilde{f}_B(\mu)\, \frac{m_B}{m_b}\, \bar{n}_\mu \int \frac{d^D l}{(2\pi)^D} \left[(2-D)\, n\cdot l\, \phi^+_{b\bar{d}}(\omega) + 2\, m_b\, \phi^-_{b\bar{d}}(\omega)\right] \times \frac{n\cdot(p+l)}{[n\cdot(p+l)\,\bar{n}\cdot(p-k+l) + l_\perp^2 + i0][n\cdot l\,\bar{n}(l-k) + l_\perp^2 + i0][l^2 + i0]}\,. \tag{51}$$

[2] No power enhanced factor can be induced for I_4 in other regions by the power counting analysis, which are therefore irrelevant here.

Using the expressions of loop integrals collected in Appendix A we obtain

$$\Pi^{(1),\,hc}_{\mu,\,box} = \frac{\alpha_s\,C_F}{4\pi}\,\tilde{f}_B(\mu)\,\frac{m_B}{\omega}\,\bar{n}_\mu\left\{\phi^+_{b\bar{d}}(\omega)\left[r\,\ln(1+\eta)\right] - 2\,\phi^-_{b\bar{d}}(\omega)\,\ln(1+\eta)\right.$$
$$\left.\times\left[\frac{1}{\epsilon} + \ln\frac{\mu^2}{n\cdot p\,(\omega-\bar{n}\cdot p)} + \frac{1}{2}\,\ln(1+\eta) + 1\right]\right\}, \tag{52}$$

with $\eta = -\omega/\bar{n}\cdot p$.

Extracting the soft contribution of $\Pi^{(1)}_{\mu,\,box}$ with the method of regions gives

$$\Pi^{(1),\,s}_{\mu,\,box} = -\frac{g_s^2\,C_F}{2}\int\frac{d^D l}{(2\pi)^D}\,\frac{1}{[v\cdot l+i0][\bar{n}\cdot(p-k+l)+i0][(k-l)^2+i0][l^2+i0]}$$
$$\bar{d}(k)\,\not{v}\,(\not{k}-\not{l})\,\not{\bar{n}}\,\gamma_5\,\not{\bar{n}}\,\gamma_\mu\,b(v)\,. \tag{53}$$

Now we compute the corresponding NLO contribution to the partonic DA (the diagram in Fig. 3c)

$$\Phi^{\alpha\beta,\,(1)}_{b\bar{d},\,c}(\omega,\omega') = -i\,g_s^2\,C_F\int\frac{d^D l}{(2\pi)^D}\,\frac{1}{[(l-k)^2+i0][v\cdot l+i0][l^2+i0]}$$
$$\times\,\delta(\omega'-\omega+\bar{n}\cdot l)\,[\bar{d}(k)\,\not{v}\,(\not{l}-\not{k})]_\alpha\,[b(v)]_\beta\,, \tag{54}$$

from which one can deduce the soft subtraction term

$$\Phi^{(1)}_{b\bar{d},\,c}\otimes T^{(0)} = \frac{g_s^2\,C_F}{2}\int\frac{d^D l}{(2\pi)^D}\,\frac{1}{[v\cdot l+i0][\bar{n}\cdot(p-k+l)+i0][(l-k)^2+i0][l^2+i0]}$$
$$\bar{d}(k)\,\not{v}\,(\not{l}-\not{k})\,\not{\bar{n}}\,\gamma_5\,\not{\bar{n}}\,\gamma_\mu\,b(v)\,, \tag{55}$$

which cancels out the soft contribution of the correlation function $\Pi^{(1),\,s}_{\mu,\,box}$ completely. The absence of such soft contribution to the perturbative matching coefficient is particularly important for the box diagram, since the relevant loop integrals in the soft region depend on *two* components of the soft spectator momentum $\bar{n}\cdot k$ and $v\cdot k$, and the light-cone OPE fails in the soft region.[3]

3.5. The hard-scattering kernel at $\mathcal{O}(\alpha_s)$

The one-loop hard-scattering kernel of the correlation function Π_μ can be readily computed from the matching condition in Eq. (19) by collecting different pieces together

$$\Phi^{(0)}_{b\bar{d}}\otimes T^{(1)} = \left[\Pi^{(1)}_{\mu,\,weak} + \Pi^{(1)}_{\mu,\,pion} + \Pi^{(1)}_{\mu,\,wfc} + \Pi^{(1)}_{\mu,\,box} + \Pi^{(1)}_{\mu,\,bwf} + \Pi^{(1)}_{\mu,\,dwf}\right]$$
$$-\left[\Phi^{(1)}_{b\bar{d},\,a} + \Phi^{(1)}_{b\bar{d},\,b} + \Phi^{(1)}_{b\bar{d},\,c} + \Phi^{(1)}_{b\bar{d},\,bwf} + \Phi^{(1)}_{b\bar{d},\,dwf}\right]\otimes T^{(0)}$$
$$= \left[\Pi^{(1),\,h}_{\mu,\,weak} + \left(\Pi^{(1)}_{\mu,\,bwf} - \Phi^{(1)}_{b\bar{d},\,bwf}\right)\right]$$
$$+\left[\Pi^{(1),\,hc}_{\mu,\,weak} + \Pi^{(1),\,hc}_{\mu,\,pion} + \Pi^{(1),\,hc}_{\mu,\,wfc} + \Pi^{(1),\,hc}_{\mu,\,box}\right], \tag{56}$$

[3] The bottom and down quarks entering the B-meson state is not light-cone separated for the soft exchanged gluon in Fig. 2d, therefore one is not allowed to use B-meson DAs to absorb the long-distance physics (i.e., non-perturbative QCD dynamics). The construction of QCD factorization itself requires decoupling of soft contributions from perturbative fluctuations in general.

where the terms in the first and second square brackets of the second equality correspond to the hard matching coefficients and the jet functions at $\mathcal{O}(\alpha_s)$. Finally, one can derive the factorization formulae of Π and $\widetilde{\Pi}$ defined in Eq. (2)

$$\begin{aligned}
\Pi &= \tilde{f}_B(\mu)\, m_B \sum_{k=\pm} C^{(k)}(n\cdot p,\mu) \int_0^\infty \frac{d\omega}{\omega-\bar{n}\cdot p}\, J^{(k)}\left(\frac{\mu^2}{n\cdot p\,\omega}, \frac{\omega}{\bar{n}\cdot p}\right) \phi_B^{(k)}(\omega,\mu)\,,\\
\widetilde{\Pi} &= \tilde{f}_B(\mu)\, m_B \sum_{k=\pm} \widetilde{C}^{(k)}(n\cdot p,\mu) \int_0^\infty \frac{d\omega}{\omega-\bar{n}\cdot p}\, \widetilde{J}^{(k)}\left(\frac{\mu^2}{n\cdot p\,\omega}, \frac{\omega}{\bar{n}\cdot p}\right) \phi_B^{(k)}(\omega,\mu)\,,
\end{aligned} \tag{57}$$

at leading power in Λ/m_b, where we keep the factorization-scale dependence explicitly, the hard coefficient functions are given by

$$\begin{aligned}
C^{(+)} &= \tilde{C}^{(+)} = 1,\\
C^{(-)} &= \frac{\alpha_s C_F}{4\pi}\frac{1}{\bar{r}}\left[\frac{r}{\bar{r}}\ln r + 1\right],\\
\tilde{C}^{(-)} &= 1 - \frac{\alpha_s C_F}{4\pi}\left[2\ln^2\frac{\mu}{n\cdot p} + 5\ln\frac{\mu}{m_b} - \ln^2 r - 2\,\mathrm{Li}_2\left(-\frac{\bar{r}}{r}\right)\right.\\
&\quad \left. + \frac{2-r}{r-1}\ln r + \frac{\pi^2}{12} + 5\right],
\end{aligned} \tag{58}$$

and the jet functions are

$$\begin{aligned}
J^{(+)} &= \frac{1}{r}\,\tilde{J}^{(+)} = \frac{\alpha_s C_F}{4\pi}\left(1-\frac{\bar{n}\cdot p}{\omega}\right)\ln\left(1-\frac{\omega}{\bar{n}\cdot p}\right),\\
J^{(-)} &= 1\,,\\
\tilde{J}^{(-)} &= 1 + \frac{\alpha_s C_F}{4\pi}\left[\ln^2\frac{\mu^2}{n\cdot p(\omega-\bar{n}\cdot p)} - 2\ln\frac{\bar{n}\cdot p-\omega}{\bar{n}\cdot p}\ln\frac{\mu^2}{n\cdot p(\omega-\bar{n}\cdot p)}\right.\\
&\quad \left. - \ln^2\frac{\bar{n}\cdot p-\omega}{\bar{n}\cdot p} - \left(1+\frac{2\bar{n}\cdot p}{\omega}\right)\ln\frac{\bar{n}\cdot p-\omega}{\bar{n}\cdot p} - \frac{\pi^2}{6} - 1\right].
\end{aligned} \tag{59}$$

Now, we verify the factorization-scale independence of Π and $\widetilde{\Pi}$ as a consequence of QCD factorization by construction. Note that the correlation function Π_μ is defined by the conserved currents in QCD, hence the ultraviolet renormalization-scale dependence of Π_μ is determined by the renormalization constant of the strong coupling constant α_s and no additional QCD operator renormalization (ultraviolet subtraction) is needed in obtaining the renormalized hard coefficients and jet functions. It is straightforward to write down the following evolution equations

$$\frac{d}{d\ln\mu}\tilde{C}^{(-)}(n\cdot p,\mu) = -\frac{\alpha_s C_F}{4\pi}\left[\Gamma^{(0)}_{\rm cusp}\ln\frac{\mu}{n\cdot p} + 5\right]\tilde{C}^{(-)}(n\cdot p,\mu)\,, \tag{60}$$

$$\begin{aligned}
\frac{d}{d\ln\mu}\tilde{J}^{(-)}\left(\frac{\mu^2}{n\cdot p\,\omega}, \frac{\omega}{\bar{n}\cdot p}\right) &= \frac{\alpha_s C_F}{4\pi}\left[\Gamma^{(0)}_{\rm cusp}\ln\frac{\mu^2}{n\cdot p\,\omega}\right]\tilde{J}^{(-)}\left(\frac{\mu^2}{n\cdot p\,\omega}, \frac{\omega}{\bar{n}\cdot p}\right)\\
&\quad + \frac{\alpha_s C_F}{4\pi}\int_0^\infty d\omega'\,\omega\,\Gamma(\omega,\omega',\mu)\,\tilde{J}^{(-)}\left(\frac{\mu^2}{n\cdot p\,\omega'}, \frac{\omega'}{\bar{n}\cdot p}\right),
\end{aligned} \tag{61}$$

$$\frac{d}{d\ln\mu}\left[\tilde{f}_B(\mu)\,\phi_B^-(\omega,\mu)\right] = -\frac{\alpha_s\,C_F}{4\pi}\left[\Gamma_{\rm cusp}^{(0)}\ln\frac{\mu}{\omega}-5\right]\left[\tilde{f}_B(\mu)\,\phi_B^-(\omega,\mu)\right]$$
$$-\frac{\alpha_s\,C_F}{4\pi}\int_0^\infty d\omega'\,\omega\,\Gamma(\omega,\omega',\mu)\,\left[\tilde{f}_B(\mu)\,\phi_B^-(\omega',\mu)\right], \tag{62}$$

where the function Γ is given by [32]

$$\Gamma(\omega,\omega',\mu) = -\Gamma_{\rm cusp}^{(0)}\,\frac{\theta(\omega'-\omega)}{\omega\,\omega'} - \Gamma_{\rm cusp}^{(0)}\left[\frac{\theta(\omega'-\omega)}{\omega'\,(\omega'-\omega)}+\frac{\theta(\omega-\omega')}{\omega\,(\omega-\omega')}\right]_\oplus \tag{63}$$

at one-loop order, with the $\oplus$ function defined as

$$\int_0^\infty d\omega'\,\left[f(\omega,\omega')\right]_\oplus\,g(\omega') = \int_0^\infty d\omega'\,f(\omega,\omega')\,\left[g(\omega')-g(\omega)\right], \tag{64}$$

and $\Gamma_{\rm cusp}^{(0)}=4$ determined by the geometry of Wilson lines. The renormalization kernel of $\phi_B^-(\omega,\mu)$ at one-loop level was first computed in [32] and then confirmed in [33]. We also mention in passing that the RG equations of both the B-meson DAs and the jet functions take a particularly simple form in the "dual" momentum space where the Lange–Neubert kernel [34] at one loop is diagonalized. More details can be found in Ref. [35] (see also [36]) and we will not pursue the discussions along this line further. With the evolution equations displayed above, it is evident that

$$\frac{d}{d\ln\mu}\left[\Pi(n\cdot p,\bar{n}\cdot p)\,,\widetilde{\Pi}(n\cdot p,\bar{n}\cdot p)\right] = \mathcal{O}(\alpha_s^2). \tag{65}$$

Inspection of Eqs. (58), (59) and (9) indicates that one cannot avoid the parametrically large logarithms of order $\ln(m_b/\Lambda_{\rm QCD})$ in the hard functions, the jet functions, $\tilde{f}_B(\mu)$ and the B-meson DAs concurrently, by choosing a common value of μ. Resummation of these logarithms to all orders of α_s can be achieved by solving the three RG equations shown above. Since the hadronic scale entering the initial conditions of the B-meson DAs $\phi_B^\pm(\omega,\mu_0)$, $\mu_0\simeq 1$ GeV, is quite close to the hard-collinear scale $\mu_{hc}\simeq\sqrt{m_b\,\Lambda_{\rm QCD}}\approx 1.5$ GeV, we will not sum logarithms of μ_{hc}/μ_0 due to the minor evolution effect [29]. Because the hard scale $\mu_{h1}\sim n\cdot p$ in the hard function $\tilde{C}^{(-)}(n\cdot p,\mu)$ differs from the one $\mu_{h2}\sim m_b$ in $\tilde{f}_B(\mu)$, the resulting evolution functions due to running of the renormalization scale from μ_{h1} (μ_{h2}) to μ_{hc} in $\tilde{C}^{(-)}$ $(n\cdot p,\mu)$ ($\tilde{f}_B(\mu)$) are

$$\tilde{C}^{(-)}(n\cdot p,\mu) = U_1(n\cdot p,\mu_{h1},\mu)\,\tilde{C}^{(-)}(n\cdot p,\mu_{h1})\,,$$
$$\tilde{f}_B(\mu) = U_2(\mu_{h2},\mu)\,\tilde{f}_B(\mu_{h2})\,. \tag{66}$$

To achieve NLL resummation of large logarithms in the hard coefficient $\tilde{C}^{(-)}$ we need to generalize the RG equation (60) to

$$\frac{d}{d\ln\mu}\tilde{C}^{(-)}(n\cdot p,\mu) = \left[-\Gamma_{\rm cusp}(\alpha_s)\ln\frac{\mu}{n\cdot p}+\gamma(\alpha_s)\right]\tilde{C}^{(-)}(n\cdot p,\mu)\,, \tag{67}$$

where the cusp anomalous dimension, $\gamma(\alpha_s)$ and the QCD β-function are expanded as

$$\Gamma_{\rm cusp}(\alpha_s) = \frac{\alpha_s C_F}{4\pi}\left[\Gamma_{\rm cusp}^{(0)} + \left(\frac{\alpha_s}{4\pi}\right)\Gamma_{\rm cusp}^{(1)} + \left(\frac{\alpha_s}{4\pi}\right)^2\Gamma_{\rm cusp}^{(2)} + \ldots\right],$$
$$\gamma(\alpha_s) = \frac{\alpha_s C_F}{4\pi}\left[\gamma^{(0)} + \left(\frac{\alpha_s}{4\pi}\right)\gamma^{(1)} + \ldots\right],$$
$$\beta(\alpha_s) = -8\pi\left[\left(\frac{\alpha_s}{4\pi}\right)^2\beta_0 + \left(\frac{\alpha_s}{4\pi}\right)^3\beta_1 + \left(\frac{\alpha_s}{4\pi}\right)^4\beta_2 + \ldots\right]. \tag{68}$$

The cusp anomalous dimension at the three-loop order and the remanning anomalous dimension $\gamma(\alpha_s)$ determining renormalization of the SCET heavy-to-light current at two loops will enter $U_1(n\cdot p, \mu_{h1}, \mu)$ at NLL accuracy. The manifest expressions of $\Gamma_{\rm cusp}^{(i)}$, $\gamma^{(i)}$ and β_i can be found in [29] and references therein,[4] the evolution function $U_1(n\cdot p, \mu_{h1}, \mu)$ can be read from Eq. (A.3) in [29] with the replacement rules $E_\gamma \to n\cdot p/2$ and $\mu_h \to \mu_{h1}$. The three-loop evolution of the strong coupling α_s in the $\overline{\rm MS}$ scheme

$$\alpha_s(\mu) = \frac{2\pi}{\beta_0}\left\{1 - \frac{\beta_1}{2\beta_0^2}\frac{\ln(2L)}{L} + \frac{\beta_1^2}{4\beta_0^4 L^2}\left[\left(\ln(2L) - \frac{1}{2}\right)^2 + \frac{\beta_2\beta_0}{\beta_1^2} - \frac{5}{4}\right]\right\},$$
$$L = \ln\left(\frac{\mu}{\Lambda_{\rm QCD}^{(n_f)}}\right) \tag{69}$$

is used with $\Lambda_{\rm QCD}^{(4)} = 229$ MeV.

The RG equation of $\tilde{f}_B(\mu)$ at the two-loop order is given by

$$\frac{d}{d\ln\mu}\tilde{f}_B(\mu) = \tilde{\gamma}(\alpha_s)\,\tilde{f}_B(\mu), \tag{70}$$

with

$$\tilde{\gamma}(\alpha_s) = \frac{\alpha_s C_F}{4\pi}\left[\tilde{\gamma}^{(0)} + \left(\frac{\alpha_s}{4\pi}\right)\tilde{\gamma}^{(1)} + \ldots\right],$$
$$\tilde{\gamma}^{(0)} = 3, \qquad \tilde{\gamma}^{(1)} = \frac{127}{6} + \frac{14\pi^2}{9} - \frac{5}{3}n_f, \tag{71}$$

where $n_f = 4$ is the number of light quark flavors. Solving this RG equation yields

$$U_2(\mu_{h2}, \mu) = {\rm Exp}\left[\int_{\alpha_s(\mu_{h2})}^{\alpha_s(\mu)} d\alpha_s\,\frac{\tilde{\gamma}(\alpha_s)}{\beta(\alpha_s)}\right]$$
$$= z^{-\frac{\tilde{\gamma}_0}{2\beta_0}C_F}\left[1 + \frac{\alpha_s(\mu_{h2})C_F}{4\pi}\left(\frac{\tilde{\gamma}^{(1)}}{2\beta_0} - \frac{\tilde{\gamma}^{(0)}\beta_1}{2\beta_0^2}\right)(1-z) + \mathcal{O}(\alpha_s^2)\right], \tag{72}$$

with $z = \alpha_s(\mu)/\alpha_s(\mu_{h2})$.

The final factorization formulae of Π and $\widetilde{\Pi}$ with RG improvement at NLL accuracy can be written as

[4] Note that there is a factor C_F difference of our conventions of $\Gamma_{\rm cusp}^{(i)}$ and $\gamma^{(i)}$ compared with [29].

$$\Pi = m_B \left[U_2(\mu_{h2},\mu)\,\tilde{f}_B(\mu_{h2})\right] \int_0^\infty \frac{d\omega}{\omega - \bar{n}\cdot p}\; J^{(+)}\left(\frac{\mu^2}{n\cdot p\,\omega}, \frac{\omega}{\bar{n}\cdot p}\right) \phi_B^{(+)}(\omega,\mu)$$
$$+ m_B \left[U_2(\mu_{h2},\mu)\,\tilde{f}_B(\mu_{h2})\right] C^{(-)}(n\cdot p,\mu) \int_0^\infty \frac{d\omega}{\omega - \bar{n}\cdot p}\; \phi_B^{(-)}(\omega,\mu)\,,$$
$$\widetilde{\Pi} = m_B \left[U_2(\mu_{h2},\mu)\,\tilde{f}_B(\mu_{h2})\right] \int_0^\infty \frac{d\omega}{\omega - \bar{n}\cdot p}\; \widetilde{J}^{(+)}\left(\frac{\mu^2}{n\cdot p\,\omega}, \frac{\omega}{\bar{n}\cdot p}\right) \phi_B^{(+)}(\omega,\mu)$$
$$+ m_B \left[U_1(n\cdot p,\mu_{h1},\mu)\,U_2(\mu_{h2},\mu)\right] \left[\tilde{f}_B(\mu_{h2})\,\widetilde{C}^{(-)}(n\cdot p,\mu_{h1})\right]$$
$$\times \int_0^\infty \frac{d\omega}{\omega - \bar{n}\cdot p}\; \widetilde{J}^{(-)}\left(\frac{\mu^2}{n\cdot p\,\omega}, \frac{\omega}{\bar{n}\cdot p}\right) \phi_B^{(-)}(\omega,\mu)\,, \tag{73}$$

where μ should be taken as a hard-collinear scale of order $\sqrt{m_b\,\Lambda}$.

3.6. Comparison with previous approaches

The aim of this subsection is to develop a better understanding of the factorization structures of Π and $\widetilde{\Pi}$ obtained above. Inspecting Eq. (56) shows that the hard-scale fluctuation of the correlation function $\Pi_\mu(n\cdot p, \bar{n}\cdot p)$ comes solely from the contributions of the weak vertex diagram and the b-quark wave function renormalization. This demonstrates that the hard matching coefficients $C^{(-)}$ and $\tilde{C}^{(-)}$ can be also extracted from the one-loop hard matching coefficients of the QCD current $\bar{q}\,\gamma_\mu\,b$ in SCET [11]

$$\bar{q}\;\gamma_\mu\;b \to \left[C_4\,\bar{n}_\mu + C_5\,v_\mu\right] \bar{\xi}_{\bar{n}}\,W_{hc}\,Y_s^\dagger\,b_v + \ldots\,, \tag{74}$$

where W_{hc} and $Y_s^\dagger$ denote the hard-collinear and soft Wilson lines, the ellipses represent terms with different Dirac structures and sub-leading power contributions. Inserting (57) into (2) and comparing with (74) gives[5]

$$C^{(-)} = \frac{1}{2}\,C_5, \qquad \tilde{C}^{(-)} = C_4 + \frac{1}{2}\,C_5\,. \tag{75}$$

The explicit expressions of C_4 and C_5 can be found in [11,12]

$$C_4 = 1 - \frac{\alpha_s\,C_F}{4\,\pi}\left[2\,\ln^2\frac{\mu}{m_b} - (4\,\ln r - 5)\,\ln\frac{\mu}{m_b} + 2\,\ln^2 r + 2\,\mathrm{Li}_2\,(1-r)\right.$$
$$\left. + \frac{\pi^2}{12} + \left(\frac{r^2}{\bar{r}^2} - 2\right)\ln r + \frac{r}{1-r} + 6\right], \tag{76}$$
$$C_5 = \frac{2}{r} + \frac{2\,r}{\bar{r}^2}\,\ln r\,, \tag{77}$$

[5] $C^{(-)}$ and $\tilde{C}^{(-)}$ correspond to the hard matching coefficients of A-type SCET currents. This can be understood from the fact that factorization of the associated SCET matrix elements involve the same DA $\phi_B^{(-)}(\omega)$ as in the tree-level approximation. $C^{(+)}$ and $\tilde{C}^{(+)}$ are the hard matching coefficients of B-type SCET currents whose matrix elements start at the first order of α_s, therefore only the tree-level contributions of $C^{(+)}$ and $\tilde{C}^{(+)}$ enter the factorization formulae of the correlation function $\Pi_\mu(n\cdot p, \bar{n}\cdot p)$ at one loop.

from which one can readily verify the relations in Eq. (75). Conceptually, this is just an example to show that perturbative coefficient functions entering QCD factorization formulae are independent of the external partonic configurations used in the matching procedure.

The jet functions $\tilde{J}^{(\pm)}$ also confront with the earlier calculations in [4] with SCET Feynman rules. It is a straightforward task to show that $\tilde{J}^{(-)}$ coincides with (2.23) in [4] while $\tilde{J}^{(+)}$ ($J^{(+)}$) is in agreement with (3.9) of [4]. A final remark is devoted to $J^{(-)}$. Because the corresponding hard coefficient $C^{(-)}$ starts at $\mathcal{O}(\alpha_s)$, only the tree-level jet function $J^{(-)}$ enters the one-loop factorization of Π_μ.

4. The LCSR for $B \to \pi$ form factors at $\mathcal{O}(\alpha_s)$

Now, we are ready to construct the sum rules of $f_{B\pi}^+(q^2)$ and $f_{B\pi}^0(q^2)$ including the radiative corrections at $\mathcal{O}(\alpha_s)$. Following the prescriptions to construct the tree-level sum rules in Section 2 and expressing the correlation function Π_μ in a dispersion form with the relations in Appendix B, we obtain

$$
\begin{aligned}
& f_\pi \; e^{-m_\pi^2/(n\cdot p\,\omega_M)} \; \left\{ \frac{n\cdot p}{m_B}\, f_{B\pi}^+(q^2)\,, \;\; f_{B\pi}^0(q^2) \right\} \\
&= \left[U_2(\mu_{h2},\mu)\, \tilde{f}_B(\mu_{h2}) \right] \int_0^{\omega_s} d\omega' \; e^{-\omega'/\omega_M} \left[r\, \phi_{B,\mathrm{eff}}^+(\omega',\mu) \right. \\
&\quad + \left[U_1(n\cdot p,\mu_{h1},\mu)\, \widetilde{C}^{(-)}(n\cdot p,\mu_{h1}) \right] \phi_{B,\mathrm{eff}}^-(\omega',\mu) \\
&\quad \left. \pm \frac{n\cdot p - m_B}{m_B} \; \left(\phi_{B,\mathrm{eff}}^+(\omega',\mu) + C^{(-)}(n\cdot p,\mu)\, \phi_B^-(\omega',\mu) \right) \right], \qquad (78)
\end{aligned}
$$

where the functions $\phi_{B,\mathrm{eff}}^{\pm}(\omega',\mu)$ are defined as

$$
\phi_{B,\mathrm{eff}}^+(\omega',\mu) = \frac{\alpha_s\, C_F}{4\pi} \int_{\omega'}^{\infty} \frac{d\omega}{\omega}\, \phi_B^+(\omega,\mu) \;, \qquad (79)
$$

$$
\begin{aligned}
\phi_{B,\mathrm{eff}}^-(\omega',\mu) &= \phi_B^-(\omega',\mu) + \frac{\alpha_s\, C_F}{4\pi} \left\{ \int_0^{\omega'} d\omega \left[\frac{2}{\omega-\omega'} \left(\ln\frac{\mu^2}{n\cdot p\,\omega'} - 2\ln\frac{\omega'-\omega}{\omega'} \right) \right]_\oplus \right. \\
&\quad \times \phi_B^-(\omega,\mu) - \int_{\omega'}^{\infty} d\omega \left[\ln^2\frac{\mu^2}{n\cdot p\,\omega'} - \left(2\ln\frac{\mu^2}{n\cdot p\,\omega'} + 3 \right) \ln\frac{\omega-\omega'}{\omega'} \right. \\
&\quad \left. \left. + 2\,\ln\frac{\omega}{\omega'} + \frac{\pi^2}{6} - 1 \right] \frac{d\phi_B^-(\omega,\mu)}{d\omega} \right\} . \qquad (80)
\end{aligned}
$$

Several comments on the structures of the sum rules are in order.

- The symmetry-breaking effects of the form-factor relation (17) can be immediately read from the last line of (78). The first term comes from the hard-collinear fluctuation and the corresponding integral is infrared finite in the heavy quark limit. One can readily confirm that this term gives an identical result of the spectator-interaction induced symmetry-breaking correction shown in Eq. (56) of [10] in the leading approximation, provided that the tree-level

sum rules of f_π in Appendix C and the asymptotic expression of the twist-2 pion DA are implemented [3]. The second term corresponds to the symmetry-breaking effect induced by the hard fluctuation and it also coincides with the second term in the bracket of Eq. (30) in [10].

- The scaling behavior of ω' in (78) is $\omega' \sim \Lambda^2/m_b$ due to the bounds of the integration, while the power counting of ω in (80) is $\mathcal{O}(\Lambda)$ determined by the canonical behaviors of the B-meson DAs $\phi_B^\pm(\omega,\mu)$. It is then evident that $\ln\left[\left(\omega-\omega'\right)/\omega'\right]$ and $\ln\left(\omega/\omega'\right)$ appeared in $\phi^-_{B,\rm eff}(\omega',\mu)$ are counted as $\ln(m_b/\Lambda)$ in the heavy quark limit. Such large logarithms are identified as the end-point divergences in QCD factorization approach (see also the discussions in [4]). However, we should also keep in mind that the NLL resummation improved hard coefficient $\left[U_1(n\cdot p,\mu_{h1},\mu)\ \widetilde{C}^{(-)}(n\cdot p,\mu_{h1})\right]$ vanishes in the heavy quark limit.

5. Numerical analysis

In this section we aim at exploring phenomenological implications of the sum rules for $f_{B\pi}^{+,0}(q^2)$ in Eq. (78) including the shapes of the two form factors, the normalized q^2 spectra of $B\to\pi\ell\nu$ for $\ell=\mu,\tau$ as well as the determinations of the CKM matrix element $|V_{ub}|$. We will first discuss the theory inputs (the B-meson DAs, the "internal" sum rule parameters, the decay constants of the B-meson and pion, etc.) entering the sum rule analysis, compute the form factors at zero momentum transfer, and then predict the shapes of $f_{B\pi}^{+,0}(q^2)$ in the small q^2 region and extrapolate the sum rule computations to the full kinematic region with the z-series parametrization.

5.1. Theory input parameters

The B-meson DAs serve as fundamental ingredients for the LCSR of the $B\to\pi$ form factors $f_{B\pi}^{+,0}(q^2)$. Albeit with the encouraging progresses in understanding their properties at large ω in perturbative QCD [37,38], our knowledge of the behaviors of $\phi_B^\pm(\omega,\mu)$ at small ω is still rather limited due to the poor understanding of non-perturbative QCD dynamics (see [39] for discussions in the context of the QCD sum rule method). To achieve a better understanding of the model dependence of $\phi_B^\pm(\omega,\mu)$ in the sum rule analysis, we consider the following four different parameterizations for the shapes of the B-meson DA $\phi_B^+(\omega,\mu_0)$:

$$
\begin{aligned}
\phi_{B,\rm I}^+(\omega,\mu_0) &= \frac{\omega}{\omega_0^2}\, e^{-\omega/\omega_0}\,,\\
\phi_{B,\rm II}^+(\omega,\mu_0) &= \frac{1}{4\pi\,\omega_0}\,\frac{k}{k^2+1}\left[\frac{1}{k^2+1}-\frac{2(\sigma_B^{(1)}-1)}{\pi^2}\ln k\right],\quad k=\frac{\omega}{1\ \text{GeV}}\,,\\
\phi_{B,\rm III}^+(\omega,\mu_0) &= \frac{2\omega^2}{\omega_0\omega_1^2}\, e^{-(\omega/\omega_1)^2},\quad \omega_1=\frac{2\,\omega_0}{\sqrt{\pi}}\,,\\
\phi_{B,\rm IV}^+(\omega,\mu_0) &= \frac{\omega}{\omega_0\omega_2}\,\frac{\omega_2-\omega}{\sqrt{\omega(2\omega_2-\omega)}}\,\theta(\omega_2-\omega)\,,\quad \omega_2=\frac{4\,\omega_0}{4-\pi}\,.
\end{aligned}
\tag{81}
$$

$\phi_{B,\rm I}^+(\omega,\mu_0)$ was originally proposed in [28] inspired by a tree-level QCD sum rule analysis. $\phi_{B,\rm II}^+(\omega,\mu_0)$ suggested in [39] was motivated from the QCD sum rule calculations at $\mathcal{O}(\alpha_s)$ with the parameter $\sigma_B^{(1)}$ defined as

$$\sigma_B^{(n)}(\mu) = \lambda_B(\mu) \int_0^\infty \frac{d\omega}{\omega} \ln^n \frac{\mu}{\omega} \phi_B^+(\omega,\mu)\,,$$

$$\lambda_B^{-1}(\mu) = \int_0^\infty \frac{d\omega}{\omega} \phi_B^+(\omega,\mu)\,. \tag{82}$$

$\phi_{B,\rm III}^+(\omega,\mu_0)$ and $\phi_{B,\rm IV}^+(\omega,\mu_0)$ are deduced from the two models of $\phi_B^-(\omega,\mu_0)$ [4] with the Wandzura–Wilczek approximation (i.e., neglecting contributions of B-meson three-particle DAs) to maximize the model dependence of $\phi_B^\pm(\omega,\mu_0)$ in theory predictions, because these two models result in the same value of λ_B as $\phi_{B,\rm I}^+(\omega,\mu_0)$ while the derivative $d\phi_B^+(\omega,\mu_0)/d\omega$ at $\omega=0$ takes extreme values 0 and ∞. The corresponding expression of $\phi_B^-(\omega,\mu_0)$ for each model is determined by the equation-of-motion constraint in the absence of contributions from three-particle DAs [10]

$$\phi_B^-(\omega,\mu_0) = \int_0^1 \frac{d\xi}{\xi} \phi_B^+\left(\frac{\omega}{\xi},\mu_0\right). \tag{83}$$

We emphasize that the above models can only provide a reasonable description of $\phi_B^\pm(\omega,\mu_0)$ at small ω due to the radiative tail developed from QCD corrections (except the second model) and the mismatch of large ω behaviors predicted from the perturbative QCD analysis [38]. Nevertheless, the dominant contributions of $f_{B\pi}^{+,0}(q^2)$ in the LCSR (78) come from the small ω region due to the strong suppression of $\phi_B^\pm(\omega,\mu_0)$ at large ω. This is also an essential prerequisite to validate QCD factorization of the correlation function Π_μ whose qualifications rely on the power counting scheme $\omega\sim\Lambda$ by construction.

As a default value, we take the factorization scale $\mu = 1.5$ GeV with a variation between 1.0 GeV and 2.0 GeV for the estimate of theory uncertainty. The scale dependence of $\lambda_B^{-1}(\mu)$ and of $\sigma_B^{(1)}(\mu)$ are governed by the following evolution equations [32,35]

$$\begin{aligned}
&\frac{d}{d\ln\mu}\lambda_B^{-1}(\mu) = -\lambda_B^{-1}(\mu)\left[\Gamma_{\rm cusp}(\alpha_s)\,\sigma_B^{(1)}(\mu) + \gamma_+(\alpha_s)\right],\\
&\frac{d}{d\ln\mu}\left[\sigma_B^{(1)}(\mu)\right] = 1 + \Gamma_{\rm cusp}(\alpha_s)\left[(\sigma_B^{(1)}(\mu))^2 - \sigma_B^{(2)}(\mu)\right],
\end{aligned} \tag{84}$$

at $\mathcal{O}(\alpha_s)$, where the anomalous dimension $\gamma_+(\alpha_s)$ is

$$\gamma_+(\alpha_s) = \frac{\alpha_s C_F}{4\pi}\left[\gamma_+^{(0)} + \left(\frac{\alpha_s}{4\pi}\right)\gamma_+^{(1)} + \ldots\right], \qquad \gamma_+^{(0)} = -2\,. \tag{85}$$

Solving these equations yields

$$\frac{\lambda_B(\mu_0)}{\lambda_B(\mu)} = 1 + \frac{\alpha_s(\mu_0) C_F}{4\pi}\ln\frac{\mu}{\mu_0}\left[2 - 2\ln\frac{\mu}{\mu_0} - 4\sigma_B^{(1)}(\mu_0)\right] + \mathcal{O}(\alpha_s^2)\,, \tag{86}$$

$$\begin{aligned}
\sigma_B^{(1)}(\mu) = {}& \sigma_B^{(1)}(\mu_0) + \ln\frac{\mu}{\mu_0}\left(1 + \frac{\alpha_s(\mu_0) C_F}{\pi}\left[(\sigma_B^{(1)}(\mu_0))^2 - \sigma_B^{(2)}(\mu_0)\right]\right)\\
&+ \mathcal{O}(\alpha_s^2)\,,
\end{aligned} \tag{87}$$

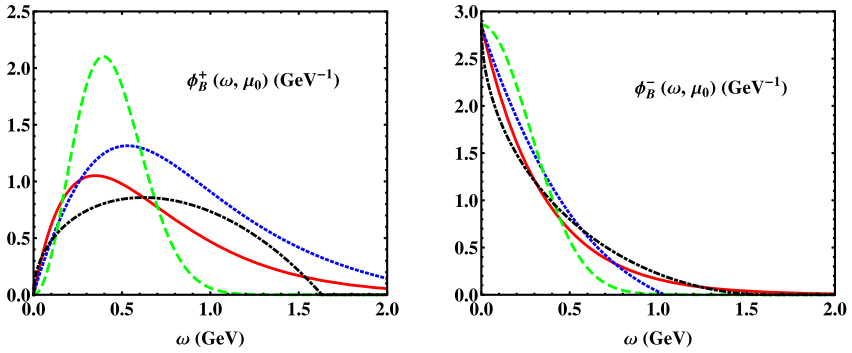

Fig. 4. Four different models of $\phi_B^+(\omega,\mu_0)$ (left plot) and $\phi_B^-(\omega,\mu_0)$ (right plot). A reference value of $\omega_0(\mu_0) = 350$ MeV is taken for all the models. Solid (red), dotted (blue), dashed (green) and dot-dashed (black) curves correspond to $\phi_{B,\mathrm{I}}^{\pm}$, $\phi_{B,\mathrm{II}}^{\pm}$, $\phi_{B,\mathrm{III}}^{\pm}$ and $\phi_{B,\mathrm{IV}}^{\pm}$, respectively. (For interpretation of the references to color in this figure legend, the reader is referred to the web version of this article.)

where we need the evolution equation of $\sigma_B^{(2)}(\mu)$ [32]

$$\frac{d}{d\ln\mu}\left[\sigma_B^{(2)}(\mu)\right] = 2\,\sigma_B^{(1)}(\mu) + \Gamma_{\mathrm{cusp}}(\alpha_s)\left[\sigma_B^{(1)}(\mu)\,\sigma_B^{(2)}(\mu) - \sigma_B^{(3)}(\mu) + 4\,\zeta_3\,\sigma_B^{(0)}(\mu)\right] + \mathcal{O}(\alpha_s^2) \tag{88}$$

to derive the second relation (87) with ζ_3 being the Riemann zeta function. As mentioned before we are not aiming at the resummation of $\ln(\mu/\mu_0)$ here. The two logarithmic moments will be taken as $\sigma_B^{(1)}(1\ \mathrm{GeV}) = 1.4 \pm 0.4$ [39] and $\sigma_B^{(2)}(1\ \mathrm{GeV}) = 3 \pm 2$ [29]. The determination of $\lambda_B(\mu_0)$, which constitutes the most important theory uncertainty in the B-meson LCSR approach, will be discussed later. Note also that we will presume the validity of the parameterizations of $\phi_B^{\pm}(\omega,\mu_0)$ in (81) at a "hard-collinear" scale of order 1.5 GeV to avoid a complicated RG evolution of $\phi_B^{\pm}(\omega,\mu)$ in the momentum space. We will first determine $\lambda_B(\mu_0)$ at a "hard-collinear" scale and then convert it to $\lambda_B(1\ \mathrm{GeV})$, using the relation in (86), for a comparison of values determined in other approaches. To illustrate the features of four models displayed in (81), numerical examples for the small ω behaviors of $\phi_B^{\pm}(\omega,\mu_0)$ at $\mu_0 = 1.5$ GeV are plotted in Fig. 4 with a reference value of $\omega_0(\mu_0) = 350$ MeV, where $\sigma_B^{(1)}(\mu_0)$ is evaluated from $\sigma_B^{(1)}(1\ \mathrm{GeV})$ with the relation in (87).

Now we turn to discuss the determinations of the Borel parameter ω_M and the effective threshold ω_s. We first recall the power counting

$$\omega_s \sim \omega_M \sim \Lambda^2/m_b\,, \tag{89}$$

in addition to which the following requirements

- The continuum contributions in the dispersion integrals of Π and $\tilde{\Pi}$ need to be less than 50%.
- The sum rules for $f_{B\pi}^{+,0}(q^2)$ are insensitive to the variation of the Borel mass ω_M. For definiteness, we impose the constraint proposed in [3]

$$\frac{\partial \ln f_{B\pi}^{+,0}}{\partial \ln \omega_M} \leq 35\%. \tag{90}$$

- The effective threshold needs to be close to that determined from the two-point correlation function with pion interpolating currents:

$$s_0 \simeq 4\pi^2 f_\pi^2 , \tag{91}$$

indicated by the parton–hadron duality.

are implemented to determine these "internal" sum rule parameters. Proceeding with the above-mentioned procedure yields

$$M^2 \equiv n\cdot p\ \omega_M = (1.25 \pm 0.25)\ \text{GeV}^2 , \qquad s_0 \equiv n\cdot p\ \omega_s = (0.70 \pm 0.05)\ \text{GeV}^2 , \tag{92}$$

in agreement with the intervals in [2].

The static decay constant $\tilde{f}_B(\mu)$ entering the sum rules (78) will be traded into the QCD decay constant f_B with the relation (9), which is evaluated from the two-point QCD sum rules at $\mathcal{O}(\alpha_s)$ as presented in Appendix C. The Borel parameter and the effective duality threshold are taken as $\overline{M}^2 = 5.0 \pm 1.0\ \text{GeV}^2$ and $\bar{s}_0 = 35.6^{+2.1}_{-0.9}\ \text{GeV}^2$ [8]. The pion decay constant f_π determined from the sum of branching ratios of $\pi^- \to \mu\bar{\nu}$ and $\pi^- \to \mu\bar{\nu}\gamma$ is $f_\pi = (130.41 \pm 0.03 \pm 0.02)$ MeV [40]. To reduce the theory uncertainties induced by the "internal" sum rule parameters we will instead use the two-point sum rules of f_π presented in Appendix C for the numerical analysis. We will return to this point later on.

A "reasonable" choice of the factorization scale is $\mu = 1.5$ GeV with the variation in the interval $1\ \text{GeV} \le \mu \le 2\ \text{GeV}$ and the hard scales μ_{h1} and μ_{h2} will be set to be equal and varied in $[m_b/2, 2m_b]$ around the default value m_b. Following [41], we adopt the bottom-quark mass in the $\overline{\text{MS}}$ scheme $\bar{m}_b(\bar{m}_b) = (4.16 \pm 0.03)$ GeV taken from [42] with a doubled uncertainly, which is still in agreement with the most recent determinations from the non-relativistic sum rules at next-to-next-to-next-to-leading order (NNNLO) [43] and from the relativistic sum rules at $\mathcal{O}(\alpha_s^3)$ [44].

5.2. Numerical results of the form factors $f_{B\pi}^{+,0}(q^2)$

Now we are in a position to discuss the inverse moment $\lambda_B(1\ \text{GeV})$ whose determination is also of central importance in the theoretical description of the radiative leptonic B-meson decays as well as the semi-leptonic and charmless hadronic B decays. Unfortunately, the favored values of $\lambda_B(1\ \text{GeV})$ implied by the hadronic B-decay data in QCD factorization [45] are not supported by the NLO QCD sum rule calculation [39] (see also [46] for a discussion). Recent searches of the radiative leptonic $B \to \ell\nu\gamma$ ($\ell = e,\ \mu$) decays from the Belle Collaboration [47] only set a boundary $\lambda_B(1\ \text{GeV}) > 238$ GeV.[6]

Given the poor knowledge of $\lambda_B(1\ \text{GeV})$ we will attempt to determine this parameter by matching the B-meson LCSR of $f_{B\pi}^+(q^2)$ at zero momentum transfer to a given input value computed from a different method. Taking $f_{B\pi}^+(0) = 0.28 \pm 0.03$ [48] evaluated from the LCSR with pion DAs (see [49] for a recent update with somewhat larger values) and proceeding with the matching procedure yields

[6] We were informed by M. Beneke that a slightly different constraint $\lambda_B(1\ \text{GeV}) > 217$ GeV is obtained with the formulae presented in [29].

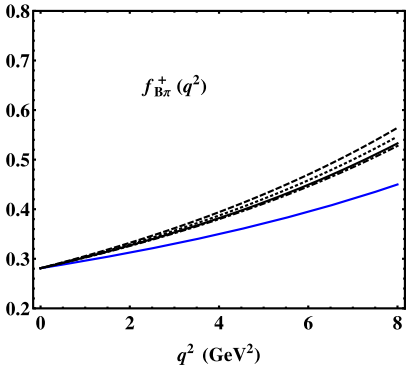

Fig. 5. The shape of $f_{B\pi}^{+}(q^2)$ with the value at zero momentum transfer fixed to the prediction from the LCSR with pion DAs, from which the parameter $\omega_0(1\ \text{GeV})$ is determined for a given model of $\phi_B^{\pm}(\omega,\mu_0)$. Solid (blue), solid (black), dotted (black), dashed (black) and dot-dashed (black) curves are obtained from the pion LCSR and from the ones with the B-meson DAs $\phi_{B,\text{I}}^{\pm}$, $\phi_{B,\text{II}}^{\pm}$, $\phi_{B,\text{III}}^{\pm}$ and $\phi_{B,\text{IV}}^{\pm}$, respectively. (For interpretation of the references to color in this figure legend, the reader is referred to the web version of this article.)

$$\begin{aligned}
&\omega_0(1\ \text{GeV}) = 354^{+38}_{-30}\ \text{MeV}\,, && \text{(Model-I)}\\
&\omega_0(1\ \text{GeV}) = 368^{+42}_{-32}\ \text{MeV}\,, && \text{(Model-II)}\\
&\omega_0(1\ \text{GeV}) = 389^{+35}_{-28}\ \text{MeV}\,, && \text{(Model-III)}\\
&\omega_0(1\ \text{GeV}) = 303^{+35}_{-26}\ \text{MeV}\,, && \text{(Model-IV)}
\end{aligned} \tag{93}$$

where the four models correspond to that shown in (81). It is evident that the extracted values of $\omega_0(1\ \text{GeV})$ are sensitive to the specific models of $\phi_B^{\pm}(\omega,\mu_0)$ entering the LCSR of $f_{B\pi}^{+,0}(q^2)$ in (78), because these sum rules cannot be controlled by the inverse moment $\lambda_B(1\ \text{GeV})$ of the DA $\phi_B^{+}(\omega,\mu_0)$ to a good approximation and the precise shapes of B-meson DAs at small ω are in demand for the sum rule analysis [4]. In other words,

$$\int_0^{\omega_s} d\omega'\, e^{-\omega'/\omega_M}\, \phi_B^{-}(\omega,\mu_0) \simeq \phi_B^{-}(\omega=0,\mu_0) \int_0^{\omega_s} d\omega'\, e^{-\omega'/\omega_M} \tag{94}$$

should *not* be taken seriously as one would expect at first sight. Mathematically, the precision of such approximation depends on the fluctuant rapidity of $\phi_B^{-}(\omega,\mu_0)$ at small ω. A similar observation was already made by inspecting the LCSR with pion DAs in the heavy quark limit [3], where the knowledge of the two lowest-order Gegenbauer moments is not sufficient to determine the key non-perturbative object $\phi_\pi'(1)$ which is highly dependent on the exact form of $\phi_\pi(u)$. We stress that the quantity $\lambda_B(\mu_0)$ itself is well defined at the operator level and is independent of the specific models of $\phi_B^{+}(\omega,\mu_0)$. A precision determination of $\lambda_B(\mu_0)$ by other means (e.g., Lattice QCD simulation) would be of great value to discriminate certain models of the B-meson DAs.

To reduce the sizeable uncertainty from modeling the B-meson DAs, we will merely aim at predicting the shape of $f_{B\pi}^{+}(q^2)$ which is insensitive to the precise behaviors of $\phi_B^{\pm}(\omega,\mu_0)$ at small ω, as displayed in Fig. 5, due to a large cancellation of the model dependence in the form-factor ratio $f_{B\pi}^{+}(q^2)/f_{B\pi}^{+}(0)$. We also find that the results of $f_{B\pi}^{+}(q^2)$ evaluated from different models of $\phi_B^{\pm}(\omega,\mu_0)$ are systematically lower than that obtained from the LCSR with pion DAs

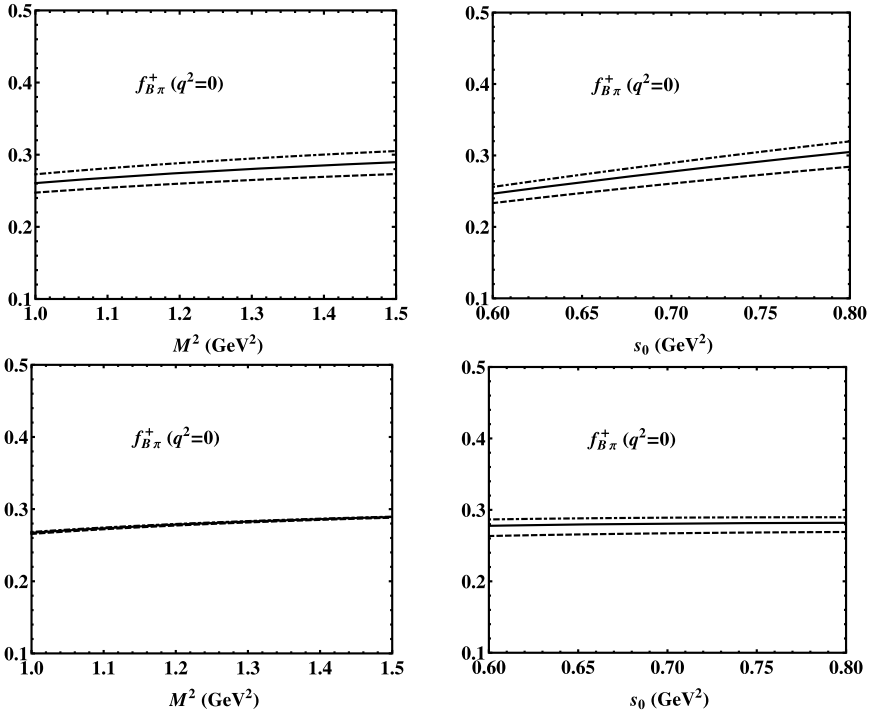

Fig. 6. Dependence of the form factor $f_{B\pi}^{+}(0)$ computed from the NLL resummation improved sum rules (78) on the Borel parameter (left panel) and on the effective threshold (right panel). The solid, dashed and dot-dashed curves correspond to $s_0 = 0.70\,\text{GeV}^2$, $0.65\,\text{GeV}^2$, $0.75\,\text{GeV}^2$ (left panel) and $M^2 = 1.25\,\text{GeV}^2$, $1.0\,\text{GeV}^2$, $1.25\,\text{GeV}^2$ (right panel), respectively.

confirming an earlier observation from the tree-level calculations [2]. The underlying mechanism responsible for such discrepancy might be due to the yet unaccounted sub-leading power corrections and/or the different ansatz of the parton–hadron duality in the constructions of sum rules, and we will return to this point later on. Hereafter, we will take $\phi_{B,\text{I}}^{\pm}(\omega,\mu_0)$ as the default model to study the implications of the sum rules in (78) and the systemic uncertainty from the model dependence of the B-meson DAs will be included in the final predictions of the two form factors $f_{B\pi}^{+,0}(q^2)$.

To demonstrate the stability of the LCSR predictions we show the dependencies of $f_{B\pi}^{+}(q^2)$ on the "internal" sum rule parameters M^2 and s_0 in Fig. 6 where the two plots on the top are obtained from NLL resummation improved sum rules (78) with f_π extracted from the experimental data as explained before; while the two-point QCD sum rules of f_π are substituted in the LCSR to produce the two plots on the bottom. One can readily find that the systematic uncertainties induced by the Borel parameter and the effective threshold are significantly reduced in the latter case, albeit with the absence of a model-independent justification of correlating the "internal" parameters in the two types of sum rules.

Now we come to investigate the factorization-scale dependence of the NLL and the leading-logarithmic (LL) resummation improved LCSR for $f_{B\pi}^{+,0}(q^2)$, where the LL predictions can be achieved by employing the cusp anomalous dimension at $\mathcal{O}(\alpha_s^2)$ as well as $\gamma(\alpha_s)$ and $\tilde{\gamma}(\alpha_s)$ at the one-loop order in the evolution functions $U_1(n\cdot p,\mu_{h1},\mu)$ and $U_2(\mu_{h2},\mu)$ of (78). Fig. 7

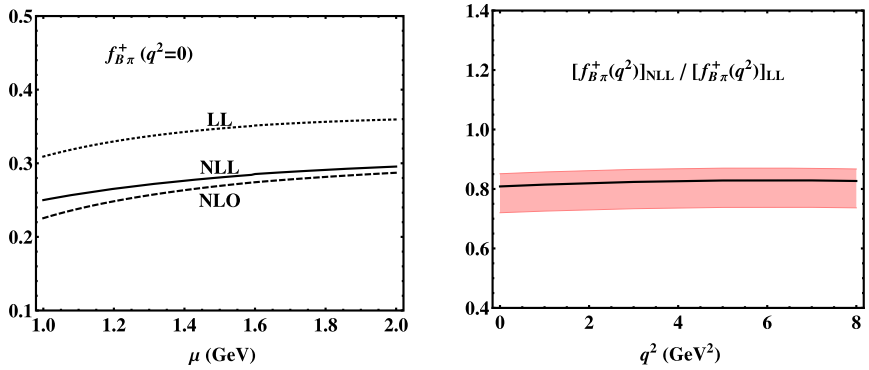

Fig. 7. Hard-collinear scale dependence of the form factor $f_{B\pi}^{+}(0)$ (left panel) and q^2 dependence of the NLO radiative correction to $f_{B\pi}^{+}(q^2)$ with both hard and hard-collinear scales varied in the allowed regions as explained in the text (right panel).

shows that the scale dependence of the NLL predictions is *not* significantly reduced compared to the LL approximation for the hard-collinear scale varied in the interval [1.0, 2.0] GeV and the discrepancy of the scale dependency for the NLL and LL predictions will be more visible for a somewhat "unrealistic" hard-collinear scale $\mu < 1.0$ GeV which is therefore excluded in the plot. The dominant radiative effect arises from the NLO QCD corrections to perturbative matching coefficients instead of resummation of the parametrically large logarithms in the heavy quark limit. However, the resummation improvement stabilizes the factorization-scale dependence in the allowed region and strengthens the predictive power of the LCSR method. One can also find that the NLO QCD correction is stable against the momentum-transfer dependence of $f_{B\pi}^{+}(q^2)$ in contrast to the case of $B \to \gamma \ell \nu$ [29].

Understanding the pion energy and the heavy quark mass dependencies of the form factors $f_{B\pi}^{+,0}(q^2)$ are of both theoretical and phenomenological interest in that different competing mechanisms appear in the theory description of heavy-to-light form factors in the large recoil region and a better control of the form factor shapes can be achieved by incorporating the energy-scaling laws and the Lattice (sum-rule) calculations of form factors at high (low) q^2. In accordance with the factorization formulae [20]

$$f_{B\pi}^{i}(E_\pi) = C_i(E_\pi)\,\xi_\pi(E_\pi) + \int d\tau\, C_i^{(B1)}(E_\pi,\tau)\,\Xi_a(\tau,E_\pi)\,,$$
$$\Xi_a(\tau,E_\pi) = \int_0^\infty d\omega \int_0^1 du\, J_\parallel(\tau,u,\omega)\,\tilde{f}_B(\mu)\,\phi_B^{+}(\omega,\mu)\,f_\pi\,\phi_\pi(u,\mu)\,, \tag{95}$$

one can readily deduce that both terms in the first line of (95) scale as $1/E_\pi^2$ in the large energy limit and as $(\Lambda/m_b)^{3/2}$ in the heavy quark limit [10,50]. It is our objective to verify such scaling behaviors from the NLL resummation improved sum rules (78). In doing so we define the following two ratios [4]

$$R_1(E_\pi) \equiv \frac{f_{B\pi}^{+}(E_\pi)}{f_{B\pi}^{+}(m_B/2)}\,, \qquad R_2(m_Q) \equiv \frac{m_Q\,\tilde{f}_B(\mu)}{m_B\,\tilde{f}_Q(\mu)}\,\frac{f_{Q\pi}^{+}(m_Q/2)}{f_{B\pi}^{+}(m_B/2)}\,, \tag{96}$$

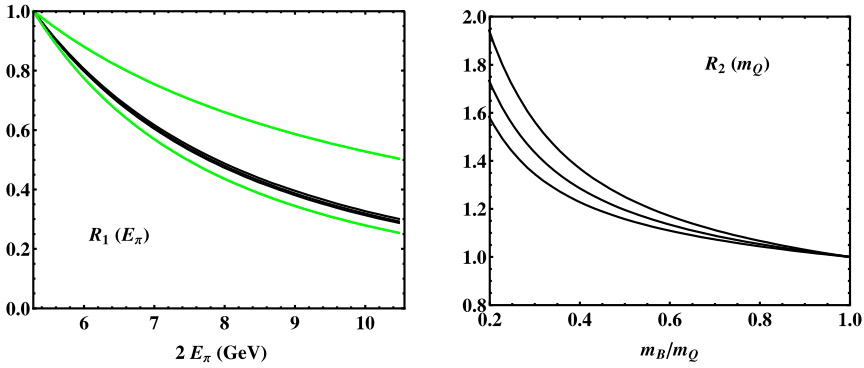

Fig. 8. Left: The pion energy dependence of the ratio $R_1(E_\pi)$. The black curves correspond to the sum rule predictions with the Borel mass taken as 1.25 GeV (solid), 1.0 GeV (dashed) and 1.5 GeV (dot-dashed). The two green curves illustrate a pure $1/E_\pi$ and a pure $1/E_\pi^2$ dependence. Right: The heavy-quark mass dependence of the quantity $R_2(m_Q)$. The three curves are predicted from the sum rules with the Borel mass varied between 1.0 GeV and 1.5 GeV around the default value 1.25 GeV. Note that in both plots we take the pion decay constant $f_\pi = 130.41$ MeV [40] instead of using the two-point QCD sum rules in Appendix C as done in the remainder of this paper. (For interpretation of the references to color in this figure legend, the reader is referred to the web version of this article.)

where the argument of the form factor refers to $n \cdot p/2$ different from that (q^2) used in the remaining of this paper, the pre-factors in the definition of $R_2(m_Q)$ is introduced to achieve a simple scaling $R_2(m_Q) \to 1$ in the heavy quark limit. The expression of $f_{Q\pi}^+(n \cdot p/2)$ can be obtained from Eq. (78) via the replacement $(m_b\,, m_B) \to (m_Q\,, m_Q)$. One should also keep in mind that the scalings of the "internal" sum rule parameters shown in (89) need to be respected when deriving the power-counting laws of the large energy and the heavy quark mass dependencies. We present the sum rule predictions for the two ratios $R_1(E_\pi)$ and $R_2(m_Q)$ in Fig. 8, where we observe that the yielding energy dependence is indeed close to the $1/E_\pi^2$ behavior and the heavy-quark mass scaling is also justified from the LCSR with B-meson DAs. However, the sum rule results become more and more instable at $m_Q > 2\,m_B$ where the Borel parameter dependence is not under control any more as displayed in Fig. 8, and one can also find that the continuum effect dominates over the ground state contribution in the dispersion integral of the correlation function Π_μ (see also the discussions in [4]).

One more comment concerns the ratio $R_2(m_Q)$ which allows to estimate $D \to \pi$ form factors from the corresponding B-meson cases in the leading-power approximation. However, this statement needs to be taken with a grain of salt in reality in view of the sizeable power correction in the decay-constant ratio f_B/f_D which is determined as

$$\frac{f_B}{f_D} = \left[\frac{m_D}{m_B}\right]^{1/2} \left[\frac{\alpha_s(m_c)}{\alpha_s(m_b)}\right]^{\frac{\tilde\gamma_0}{2\beta_0} C_F} \left\{1 + \frac{[\alpha_s(m_b) - \alpha_s(m_c)]\, C_F}{4\pi} \times \left[-2 + \left(\frac{\tilde\gamma^{(1)}}{2\beta_0} - \frac{\tilde\gamma^{(0)}\beta_1}{2\beta_0^2}\right)\right]\right\}$$
$$\simeq 0.69\,, \tag{97}$$

significantly lower than the QCD sum rule prediction $0.93 \le f_B/f_D \le 1.19$ [51] and the Lattice QCD result computed from $f_B = (190.5 \pm 4.2)$ MeV and $f_D = (209.3 \pm 3.3)$ MeV with $N_f = 2 + 1$ [52].

To validate the light-cone expansion of the correlation function Π_μ in the region $|\bar{n}\cdot p| \sim \mathcal{O}(\Lambda)$ we need to keep the photon energy as a hard scale, above the practical value of a hard-collinear scale ~ 1.5 GeV, then the LCSR with B-meson DAs can be trusted at $q^2 \leq q^2_{max} = 8\ \text{GeV}^2$ (see [2] for more detailed discussions) on the conservative side. To extrapolate the computed form factors from the LCSR method at large recoil toward large momentum transfer q^2 we apply the z-series parametrization based upon the analytical and asymptotic properties of the form factors, where the entire cut q^2-plane is mapped onto the unit disk $|z(q^2, t_0)| < 1$ via the conformal transformation

$$z(q^2, t_0) = \frac{\sqrt{t_+ - q^2} - \sqrt{t_+ - t_0}}{\sqrt{t_+ - q^2} + \sqrt{t_+ - t_0}}, \tag{98}$$

where $t_+ = (m_B + m_\pi)^2$ denotes the threshold of continuum states in the $B^*(1^-)$ meson channel. The free parameter $t_0 \in (-\infty, t_+)$ determines the value of q^2 mapped onto the origin in the z plane and can be adjusted to minimize the z interval from mapping the LCSR region $q^2_{min} \leq q^2 \leq q^2_{max}$. For definiteness, we follow [48]

$$t_0 = t_+^2 - \sqrt{t_+ - t_-}\sqrt{t_+ - q^2_{min}}, \tag{99}$$

with $q^2_{min} = -6.0\ \text{GeV}^2$ and $t_- \equiv (m_B - m_\pi)^2$, and we also refer to [48,53] and the references therein for more discussions on different versions of the z-parametrization and to [49] for a new implementation of the unitary bounds for the vector $B \to \pi$ form factor.

Employing the z-series expansion and taking into account the threshold t_+ behavior implies the following parametrization of the vector form factor [48]

$$f^+_{B\pi}(q^2) = \frac{f^+_{B\pi}(0)}{1 - q^2/m^2_{B^*}}\left\{1 + \sum_{k=1}^{N-1} b_k \left(z(q^2, t_0)^k - z(0, t_0)^k - (-1)^{N-k}\frac{k}{N}\left[z(q^2, t_0)^N - z(0, t_0)^N\right]\right)\right\}, \tag{100}$$

where the expansion coefficients b_k can be determined by matching the computed $f^+_{B\pi}(q^2)$ at low q^2 onto Eq. (100) and we truncate the z-series at $N = 2$ in the practical calculation. One can keep more terms of the z expansion in the fitting program to quantify the systematic uncertainty induced by the truncation, however, one could also run the risk of increasingly unconstrained fit when introducing too many parameters [54], and we will leave a refined statistic analysis for the future. Along this line, one can further parameterize the scalar form factor as

$$f^0_{B\pi}(q^2) = f^0_{B\pi}(0)\left\{1 + \sum_{k=1}^{N} \tilde{b}_k \left(z(q^2, t_0)^k - z(0, t_0)^k\right)\right\}, \tag{101}$$

where the pole factor is removed because the lowest scalar $B(0^+)$ meson is located above the continuum cut t_+, and the series is truncated at $N = 1$ with $f^0_{B\pi}(0) = f^+_{B\pi}(0)$ by definition. We also implement the unitary bound constraints on the coefficients of b_k and $\tilde{b}_k$ in the fitting program, which are however too weak to take effect for the truncation at $N = 2$ for $f^+_{B\pi}(q^2)$ and at $N = 1$ for $f^0_{B\pi}(q^2)$.

Fig. 9 shows the q^2 dependence of the two form factors $f^{+,0}_{B\pi}(q^2)$ computed from the LCSR with B-meson DAs at $q^2 < 8\ \text{GeV}^2$ with an extrapolation to $q^2 = 12\ \text{GeV}^2$ (pink band) using

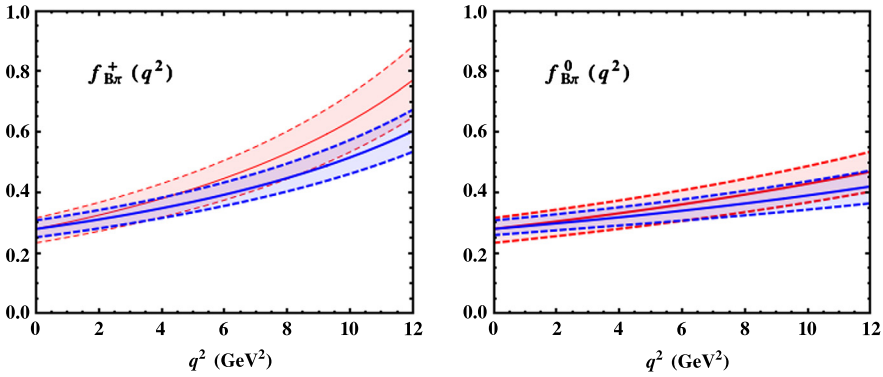

Fig. 9. q^2 dependence of the vector form factor $f^+_{B\pi}(q^2)$ (left) and of the scalar form factor $f^0_{B\pi}(q^2)$ (right). The pink (solid) and the blue (solid) curves are computed from the LCSR with B-meson DAs and with pion DAs, respectively, and the shaded regions indicate the estimated uncertainties. (For interpretation of the references to color in this figure legend, the reader is referred to the web version of this article.)

the z expansion, and theoretical predictions from the LCSR with pion DAs [48] *without* any extrapolation at $q^2 < 12\,\text{GeV}^2$ (blue band) are also presented for a comparison. It is evident that the predict shape of $f^0_{B\pi}(q^2)$ is in good agreement with that computed from the sum rules with pion DAs while a similar comparison for the vector form factor $f^+_{B\pi}(q^2)$ reveals perceptible discrepancies in particular at high q^2 as already observed before.

As the first attempt to understand this issue it would be interesting to inspect influence of the matching condition of $\omega_0(1\,\text{GeV})$, described before Eq. (93), on the final predictions of the form-factor shapes. Taking $f^+_{B\pi}(17.34\,\text{GeV}^2) = 0.94^{+0.06}_{-0.07}$ from Fermilab/MILC Collaborations [55] as an input and proceeding with the matching procedure we obtain $\omega_0(1\,\text{GeV}) = 525 \pm 29\,\text{MeV}$ for the default model of $\phi_B^{\pm}(\omega, \mu_0)$, which is significantly larger than the determinations displayed in (93). The resulting shape of the re-scaled form factor $(1 - q^2/m^2_{B^*})\, f^+_{B\pi}(q^2)$ is presented in Fig. 10 where the Lattice data from HPQCD Collaboration [56], RBC/UKQCD Collaborations [57] and Fermilab/MILC Collaborations [55] are also displayed for a comparison. One can readily observe that the higher q^2 shape of $f^+_{B\pi}(q^2)$ predicted by Fermilab/MILC [55] lies in between that obtained from the LCSR with B-meson DAs and the one with pion DAs. In fact, the recent Lattice calculations [55] (see Fig. 24 there) already revealed a faster growing form factor $f^+_{B\pi}(q^2)$ in the momentum transfer squared compared to that computed from the LCSR with pion DAs. We should stress that the new matching procedure discussed here needs to be interpreted more carefully, because extrapolating the sum rule computations toward large momentum transfer with the z expansion is also implemented for the sake of determining $\omega_0(1\,\text{GeV})$ from the Lattice input at a high $q^2 = 17.34\,\text{GeV}^2$.

We present the fitted values of $f^+_{B\pi}(0)$ and of the slop parameters b_1 and $\tilde{b}_1$ in Table 1 where breakdown of the numerically important uncertainties is also shown. A few comments on the numerical results obtained above are in order.

- The very limited information of $\phi_B^{\pm}(\omega)$ (indicated by the variations of ω_0 and by the model dependence of $\phi_B^{\pm}(\omega)$ in the table) remains the most significant source of theory uncertainties.

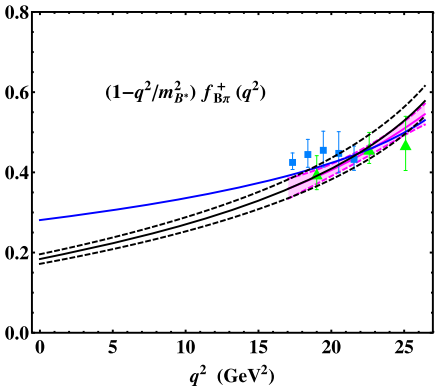

Fig. 10. q^2 dependence of the re-scaled form factor $(1-q^2/m_{B^*}^2)\, f_{B\pi}^+(q^2)$ predicted from the sum rules with B-meson DAs and the parameter $\omega_0(1\,\text{GeV})$ determined by matching the Lattice point at $q^2 = 17.34\,\text{GeV}^2$ [55]. The Lattice data are taken from Fermilab/MILC [55] (pink band), HPQCD [56] (blue squares), RBC/UKQCD [57] (green triangles). The blue curve is again obtained from the sum rules with pion DAs [48] with central inputs. (For interpretation of the references to color in this figure legend, the reader is referred to the web version of this article.)

Table 1
Fitted values of the form factor $f_{B\pi}^+(q^2)$ at zero momentum transfer and of the slop parameters b_1, $\tilde{b}_1$ entering the z expansions (100) and (101). The notation "default" means that all the parameters are taken as the central values in the numerical evaluation. Note that the central value of $f_{B\pi}^+(0)$ is taken from [48] to determine $\omega_0(1\,\text{GeV})$ from the matching condition, whose variations induce the combined uncertainty estimated in [48] by construction. Negligible uncertainties induced by variations of the remaining parameters are not shown but are taken into account in the combined uncertainty.

Parameter	Default	ω_0	$\sigma_B^{(1)}$	μ	$\mu_{h1(2)}$	$\{M^2, s_0\}$	$\{\overline{M}^2, \overline{s}_0\}$	$\phi_B^{\pm}(\omega)$
$f_{B\pi}^+(0)$	0.281	$^{-0.029}_{+0.027}$	$^{-0.008}_{+0.008}$	$^{+0.015}_{-0.031}$	$^{+0.005}_{-0.004}$	$^{+0.008}_{-0.014}$	$^{+0.012}_{-0.007}$	–
b_1	−3.92	$^{-0.10}_{+0.09}$	$^{-0.03}_{+0.03}$	$^{+0.06}_{-0.00}$	$^{-0.01}_{+0.06}$	$^{+0.08}_{-0.09}$	–	$^{+0.14}_{-0.95}$
$\tilde{b}_1$	−5.37	$^{-0.13}_{+0.12}$	$^{-0.03}_{+0.03}$	$^{+0.21}_{-0.41}$	$^{+0.05}_{-0.00}$	$^{+0.11}_{-0.12}$	–	$^{+0.17}_{-1.15}$

- Comparing the new predictions in Table 1 with that of [48] we notice again the greater slop parameters for both the vector and scalar form factors determined by the LCSR with B-meson DAs.
- Since the prediction of $f_{B\pi}^+(0)$ from the LCSR with pion DAs is taken as an input to determine the inverse moment $\lambda_B(1\,\text{GeV})$ and resummation of large logarithms in the hard function $\tilde{C}^{(-)}$ is implemented in the B-meson LCSR, theory uncertainties of the slop parameters b_1 and $\tilde{b}_1$ in Table 1 are comparable to that presented in [48] where the scale variation induces sizeable errors. However, one should keep in mind that power suppressed contributions induced by the higher twist pion DAs are taken into account in the traditional LCSR calculations [8]; while power suppressed effects to the B-meson LCSR generated by the sub-leading B-meson DAs and/or the sub-dominant hard scattering kernels are not included in the current analysis. In addition, we do not consider the correlation between the normalization and the slop parameters of the form factors as carried out in the LCSR with pion DAs [49].

5.3. $|V_{ub}|$ and the normalized q^2 distributions of $B \to \pi \ell \nu_\ell$

The CKM matrix element $|V_{ub}|$ can be determined from the (partial) branching fraction of $B \to \pi \ell \nu_\ell$

$$\frac{d\Gamma}{dq^2}(B \to \pi \ell \nu_\ell) = \frac{G_F^2 |V_{ub}|^2}{24\pi^3 q^4 m_B^2}(q^2 - m_l^2)^2 |\vec{p}_\pi| \left[\left(1 + \frac{m_l^2}{2q^2}\right) m_B^2 |\vec{p}_\pi|^2 |f_{B\pi}^+(q^2)|^2 + \frac{3m_l^2}{8q^2}(m_B^2 - m_\pi^2)^2 |f_{B\pi}^0(q^2)|^2 \right], \tag{102}$$

where $|\vec{p}_\pi|$ is the magnitude of the pion three-momentum in the B-meson rest frame, and in the massless lepton limit the above equation can be reduced to

$$\frac{d\Gamma}{dq^2}(B \to \pi \mu \nu_\mu) = \frac{G_F^2 |V_{ub}|^2}{24\pi^3} |\vec{p}_\pi|^3 |f_{B\pi}^+(q^2)|^2 . \tag{103}$$

Following [48] we define the following quantity

$$\Delta\zeta(0, q_0^2) = \frac{G_F^2}{24\pi^3} \int_0^{q_0^2} dq^2 |\vec{p}_\pi|^3 |f_{B\pi}^+(q^2)|^2 , \tag{104}$$

which allows a straightforward extraction of $|V_{ub}|$ when compared to experimental measurements for the partial branching ratio of $B \to \pi \mu \nu_\mu$ integrated over the same kinematic region. Implementing the computed form factor $f_{B\pi}^+(q^2)$ from the sum rules with B-meson DAs and performing the extrapolation to $q^2 = 12\ \text{GeV}^2$ with the z-series parametrization yield

$$\begin{aligned}\Delta\zeta(0, 12\ \text{GeV}^2) &= 5.89\ {}^{+1.12}_{-1.10}\Big|_{\omega_0}\ {}^{+0.30}_{-0.29}\Big|_{\sigma_B^{(1)}}\ {}^{+0.60}_{-1.22}\Big|_{\mu}\ {}^{+0.21}_{-0.21}\Big|_{\mu_{h1(2)}}\ {}^{+0.34}_{-0.53}\Big|_{M,s_0}\ {}^{+0.52}_{-0.25}\Big|_{\overline{M},\overline{s}_0}\ \text{ps}^{-1} \\ &= 5.89^{+1.63}_{-1.82}\ \text{ps}^{-1} ,\end{aligned} \tag{105}$$

where the negligibly small uncertainties from variations of the remaining parameters are not presented but are included in the final combined uncertainty.

Employing experimental measurements of the integrated branching ratio

$$\Delta\mathcal{BR}(0, q_0^2) = |V_{ub}|^2 \Delta\zeta(0, q_0^2) \tag{106}$$

of the semi-leptonic $\bar{B}^0 \to \pi^+ \mu \nu_\mu$ decay [58,59]:

$$\begin{aligned}\Delta\mathcal{BR}(0, 12\ \text{GeV}^2) &= (0.83 \pm 0.03 \pm 0.04) \times 10^{-4} , \qquad \text{[BaBar 2012]} \\ \Delta\mathcal{BR}(0, 12\ \text{GeV}^2) &= (0.808 \pm 0.062) \times 10^{-4} , \qquad \text{[Belle 2013]}\end{aligned} \tag{107}$$

and taking the mean lifetime $\tau_{B^0} = (1.519 \pm 0.005)$ ps [40] we obtain

$$|V_{ub}| = \left(3.05^{+0.54}_{-0.38}|_{\text{th.}} \pm 0.09|_{\text{exp.}}\right) \times 10^{-3} , \tag{108}$$

where the reduction of $|V_{ub}|$ compared to [48] is attributed to the rapidly increasing form factor $f_{B\pi}^+(q^2)$, with respect to q^2, computed from the sum rules with B-meson DAs, and the diminishing $\Delta\mathcal{BR}(0, 12\ \text{GeV}^2)$ from the new measurements [58,59] in relative to the previous BaBar measurements [60,61]; the theoretical uncertainty is from the computation of $\Delta\zeta(0, 12\ \text{GeV}^2)$ as displayed in (105).

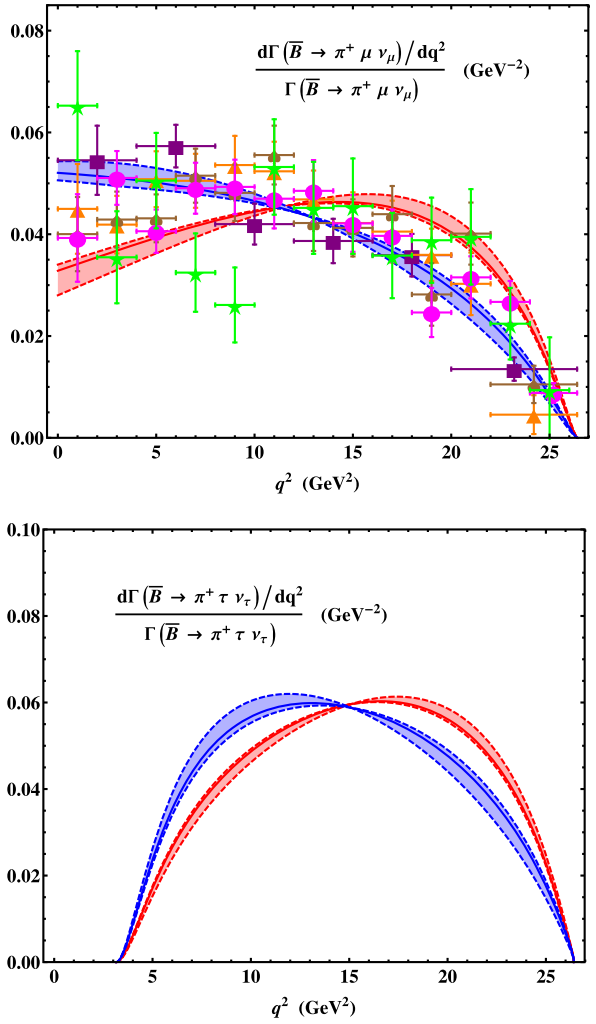

Fig. 11. Top: The normalized differential q^2 distribution of $B \to \pi\mu\nu_\mu$ computed from (103) with the form factor $f_{B\pi}^+(q^2)$ predicted from the sum rules with B-meson DAs and fitted to the z-parametrization (red band), and that predicted from the sum rules with pion DAs and z-parametrization (blue band). The experimental data bins are taken from [58] (brown spade suits), [59] (green five-pointed stars), [60] (purple squares), [61] (orange triangles), [62] (magenta full circles). Bottom: The normalized differential distribution of $B \to \pi\tau\nu_\tau$. The red and blue bands are obtained with the form factors computed from the B-meson LCSR and from the pion LCSR, respectively. (For interpretation of the references to color in this figure legend, the reader is referred to the web version of this article.)

Now we turn to compute the normalized differential q^2 distributions of $B \to \pi\ell\nu_\ell$ using the form factors obtained with the B-meson LCSR and extrapolated with the z-series parametrization. Our predictions of the normalized q^2 distribution are plotted in Fig. 11 where the available data from BaBar and Belle Collaborations are also shown for a comparison. We observe a reasonable agreement of our predictions for the q^2 distribution of $B \to \pi\mu\nu_\mu$ and the new Belle and BaBar data points [58,59], but a poor agreement when confronted with the previous measurements [60–62] in particular in the low q^2 region. It is evident that the theory uncertainty of the normalized differential distribution of $B \to \pi\mu\nu_\mu$ is somewhat smaller than that of the form

factors shown in Fig. 9 because of the partial cancellation in the ratio of the differential and the total branching ratio with respect to the variations of theory inputs. The q^2 shape of the normalized distribution for $B \to \pi \mu \nu_\mu$ is also confronted with the prediction from the pion LCSR in [48]. As a by-product, we further plot the normalized differential distribution of $B \to \pi \tau \nu_\tau$ in Fig. 11, which provides an independent way to extract $|V_{ub}|$ with the aid of future measurements at the Belle-II experiment.

6. Three-particle DAs of the B meson

We have not touched three-parton Fock-state contributions to the form factors $f_{B\pi}^{+,0}(q^2)$ in the context of the LCSR with B-meson DAs. This topical problem has triggered "sophisticated" discussions in the literature from different perspectives, see [21,63–66] for an incomplete list. We will first make some general comments on non-valence Fock state contributions to $B \to \pi$ form factors, and then discuss how B-meson three-particle DAs could contribute to the sum rules presented in this work briefly.

- The representation of the heavy-to-light currents in the context of SCET (c, s) indicates that three-parton Fock-state contributions already appear at leading power in Λ/m_b [21] and these contributions preserve the large-recoil symmetry relations at leading power albeit with the emergence of endpoint divergences [21,63]. This observation was confirmed independently by QCD sum rule calculations of $B \to \pi$ form factors with pion DAs [64].
- The tree-level contribution of three-particle DAs in $B \to \pi$ form factors is of minor importance numerically (at percent level) confirmed by two different types of sum rules with B-meson DAs [2] and with pion DAs [8], respectively. The insignificant tree-level effect can be understood transparently from the sum rules with pion DAs, where the collinear gluon emission from the b-quark propagator yields power suppression in Λ/m_b. However, this power-suppression mechanism will be removed at $\mathcal{O}(\alpha_s)$, because the radiative gluon can be emitted from the (hard)-collinear light-quark propagators in the evaluation of the corresponding correlation function at NLO (for a concrete example, see [64]). A complete calculation of three-parton Fock-state contributions to $B \to \pi$ form factors is unfortunately not available in the framework of both sum rule approaches at present. In the following we will sketch this absorbing and challenging calculation in the context of the LCSR with B-meson DAs.
- B-meson three-particle DAs could manifest themselves in the NLO sum rules in a variety of ways. First, these contributions are essential to compensate the factorization-scale dependence of $\phi_B^-(\omega,\mu)$ entering the factorization formulae of $\Pi(n\cdot p\,, \bar n\cdot p)$ and $\tilde\Pi(n\cdot p\,, \bar n\cdot p)$ at $\mathcal{O}(g_s^3)$ recalling the evolution equation [33]

$$\begin{aligned}\frac{d}{d\ln\mu}\,\phi_B^-(\omega,\mu) = -\frac{\alpha_s\, C_F}{4\pi}\Bigg\{&\left[\Gamma_{\rm cusp}^{(0)}\ln\frac{\mu}{\omega}-2\right]\phi_B^-(\omega,\mu)\\ &+\int_0^\infty d\omega'\,\omega\,\Gamma(\omega,\omega',\mu)\,\phi_B^-(\omega,\mu)\\ &+\int_0^\infty d\omega'\int_0^\infty d\xi'\,\gamma_{-,3}^{(1)}(\omega,\omega',\xi',\mu)\,[\Psi_A-\Psi_V](\omega',\xi',\mu)\Bigg\},\end{aligned} \tag{109}$$

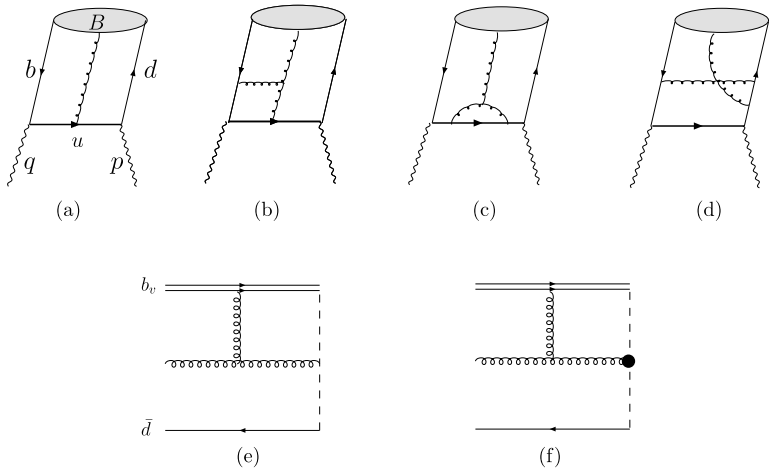

Fig. 12. Top: Contributions of B-meson three-particle DAs to the correlation function Π_μ at tree level (the diagram (a)) and at one-loop order (typical diagrams displayed in (b), (c) and (d)). Bottom: Typical diagrams for renormalization of two-parton (the diagram (e)) and three-parton (the diagram (f)) DAs at $\mathcal{O}(g_s^3)$. The black blob in the diagram (f) indicates the external gluon field in the string operator defining three particle DAs of the B-meson.

where the mixing term is solely governed by the light degrees of freedom in the composite operator [67]. A sample diagram is shown in Fig. 12(b) whose soft divergences can be reproduced by adding up amplitudes of the two effective diagrams displayed in Figs. 12(e) and 12(f) convoluted with the corresponding tree-level hard-scattering kernel. Second, B-meson three-particle DAs can induce leading-power contributions without recourse to the above-mentioned mixing pattern and one also expects that the soft subtraction is not needed here due to power suppression of the tree-level contribution from three-particle DAs. One should notice that renormalization of B-meson three-particle DAs will not generate the inverse mixing into two-particle DAs, at least, at $\mathcal{O}(\alpha_s)$, while a similar statement holds to all orders of α_s for pion DAs due to conformal symmetry [68]. Third, three-particle DAs can revise the Wandzura–Wilczek relation (83) which needs to be generalized into [35]

$$\omega\,\phi_B^-(\omega) - \int_0^\omega d\eta\,\big[\phi_B^-(\eta) - \phi_B^+(\eta)\big] = 2\int_0^\omega d\eta \int_{\omega-\eta}^\infty \frac{d\xi}{\xi}\,\frac{\partial}{\partial\xi}\big[\Psi_A(\eta,\xi) - \Psi_V(\eta,\xi)\big]\,. \tag{110}$$

7. Conclusions and discussion

We have carried out, for the first time, perturbative corrections to $B \to \pi$ form factors from the QCD LCSR with B-meson DAs proposed in [1,2] where the sum rules for heavy-to-light form factors were established at tree level including contributions from both two-particle and three-particle DAs. We placed particular emphasis on the demonstration of factorization of the vacuum-to-B-meson correlation function $\Pi_\mu(n\cdot p, \bar{n}\cdot p)$ at $\mathcal{O}(\alpha_s)$ taking advantage of the method of regions which allows a transparent separation of different leading regions with the

aid of the power counting scheme. Precise cancellation of the soft contribution to the correlation function Π_μ and the infrared subtraction was perspicuously shown at the diagrammatic level. The short-distance function obtained with integrating out the hard-scale fluctuation receives the contribution from the weak-vertex diagram solely because the loop integrals from the remaining diagrams do not involve any external invariant of order 1. The resulting hard coefficients coincide with the corresponding matching coefficients of the vector QCD weak current in $\mathrm{SCET_I}$ indicating that perturbative coefficients in the OPE are independent of the external partonic configuration chosen in the matching procedure as expected. The computed jet functions from integrating out dynamics of the hard-collinear scale are also in agreement with the expressions derived from the SCET Feynman rules [3]. We further verified factorization-scale independence of the correlation function at $\mathcal{O}(\alpha_s)$ employing evolution equations of the hard function $\tilde{C}^{(-)}$, the jet function $\tilde{J}^{(-)}$ and the B-meson DA $\phi_B^-(\omega,\mu)$, then summed up the large logarithms due to the appearance of distinct energy scales by the standard RG approach in the momentum space. We left out resummation of the parametrically large logarithms of μ_{hc}/μ_0 due to the insignificance numerically. However, there is no difficulty to achieve this resummation whenever such theory precision is in demand and an elegant way to perform resummation of large logarithms in the presence of the cusp anomalous dimension in the evolution equations is to work in the "dual" momentum space where the Lange–Neubert kernel of the B-meson DAs are diagonalized [35].

With the resummation improved sum rules (78) at hand, we explored their phenomenological implications on $B\to\pi$ form factors at large hadronic recoil in detail. Due to our poor knowledge of the inverse moment of the B-meson DA $\phi_B^+(\omega,\mu)$ we first determine this parameter by matching the B-meson LCSR prediction of $f_{B\pi}^+(q^2)$ at zero momentum transfer to the result obtained from the sum rules with pion DAs at NLO, utilizing four different models of $\phi_B^\pm(\omega,\mu)$ displayed in (81). While these models do not capture the features of large ω behaviors from perturbative QCD analysis, the power counting rule $\omega\sim\Lambda$, thanks to the canonical picture of the B-meson bound state, implemented in the construction of QCD factorization for the correlation function Π_μ requires that the dominant contribution in the factorized amplitude must be from the small ω region. We then found that the obtained values of the shape parameter $\omega_0(1\,\mathrm{GeV})$ from the matching procedure are rather sensitive to the shapes of $\phi_B^\pm(\omega,\mu)$ at small ω, pointing to the poor "local" approximation (94) and confirming an earlier observation made in [4]. However, the q^2 shape of $f_{B\pi}^+(q^2)$ predicted from LCSR is insensitive to the specific model of the B-meson DAs after determining $\omega_0(1\,\mathrm{GeV})$ from the above-described matching condition. This is not surprising because of a large cancellation of the theory uncertainty in the form-factor ratio $f_{B\pi}^+(q^2)/f_{B\pi}^+(0)$. Moreover, we showed that the dominating radiative effect originates from the NLO QCD correction instead of the NLL resummation of large logarithms in the heavy quark limit, which does however improve the stability of varying the factorization scale. Proceeding with the resummation improved sum rules (78) in the large recoil region, $q^2\le 8\,\mathrm{GeV}^2$, and extrapolating the computed from factors toward large momentum transfer, we found that the obtained scalar form factor $f_{B\pi}^0(q^2)$ is in a reasonable agreement with that from the LCSR with pion DAs at $q^2\le 12\,\mathrm{GeV}^2$; while a similar comparison of the vector form factor $f_{B\pi}^+(q^2)$ calculated from two different sum rule approaches reveals noticeable discrepancies particularly at higher q^2. We made a first step towards understanding this intriguing problem by determining the parameter $\omega_0(1\,\mathrm{GeV})$ from matching the form factor $f_{B\pi}^+(13.74\,\mathrm{GeV}^2)$ to the Lattice data from Fermilab/MILC Collaborations. It was then shown that the shape of $f_{B\pi}^+(q^2)$ at high q^2 predicted from Lattice QCD simulation lies

in between that obtained from the two sum rule approaches. It remains unclear whether the observed discrepancies arise from the sub-leading power contributions to both LCSR and/or from the systematic uncertainties induced by different kinds of parton–hadron duality relations in the constructions of sum rules and/or from the yet unknown leading-power contribution from three-particle DAs in both approaches. As a result of the rapidly growing form factor $f_{B\pi}^{+}(q^2)$ we obtain lower values of $|V_{ub}| = \left(3.05^{+0.54}_{-0.38}|_{\rm th.} \pm 0.09|_{\rm exp.}\right) \times 10^{-3}$, in contrast to the predictions of the pion LCSR [48,49], by comparing BaBar and Belle measurements of the integrated branching ratio of $B \to \pi\,\mu\,\nu_\mu$ in the region $0 < q^2 < 12\,{\rm GeV}^2$ with the computed quantity $\Delta\zeta(0, 12\,{\rm GeV}^2)$ in (105). The theory uncertainty is dominated by the rather limited information of the B-meson DAs at small ω encoding formidable (non-perturbative) strong-interaction dynamics. Precision measurements of the differential q^2 distributions of $B \to \pi\ell\nu_\ell$ ($\ell = \mu, \tau$) at the Belle-II experiment might shed light on the promising orientation to resolve the tension of the form factor shapes and subsequently to put meaningful constraints on the small ω behaviors of $\phi_B^{\pm}(\omega)$.

We further turned to discuss non-valence Fock-state contributions to the form factors $f_{B\pi}^{+,0}(q^2)$, which are the missing ingredients of our computations, and to illustrate modifications of the sum rule analysis in the presence of three-particle DAs of the B meson. Given the fact that non-valence Fock-state contributions to the form factors $f_{B\pi}^{+,0}(q^2)$ are either suppressed in powers of Λ/m_b at tree level or suppressed by the QCD coupling constant α_s at NLO, one may expect that including three-particle DAs of the B meson may generate a modest effect on the form-factor predictions albeit with a high demand of computing their contributions at $\mathcal{O}(\alpha_s)$ in the conceptual aspect.

Developing the LCSR of $B \to \pi$ form factors with B-meson DAs beyond this work can be pursued further by including the sub-leading power contributions of the considered correlation function, which requires better knowledge of the sub-leading DAs of the B meson (e.g., off-light-cone corrections) and demonstrations of factorization for the correlation function at sub-leading power in Λ/m_b. Computing yet higher order QCD corrections of the correlation function would be also interesting conceptually, but one would need the two-loop evolution equation of $\phi_B^{-}(\omega, \mu)$, which can be complicated by more involved mixing of string operators under renormalization.[7]

Moreover, we also expect phenomenological extensions of this work to compute NLO QCD corrections of many other hadronic matrix elements from the LCSR with bottom-hadron DAs. First, it is of interest to perform a comprehensive analysis of $B \to P, V$ form factors with $P = \pi, K$ and $V = \rho, K^*$ from the B-meson LCSR at $\mathcal{O}(\alpha_s)$, which serve as fundamental theory inputs for QCD factorization of the electro-weak penguin $B \to K^{(*)}\,\ell\ell$ decays and the charmless hadronic $B \to PP$ and $B \to PV$ decays. In particular, such analysis could be of value to understand the tension of form-factor ratios between the traditional LCSR and QCD factorization firstly observed in [10], keeping in mind that these ratios are less sensitive to the shapes of B-meson DAs at small ω. Second, a straightforward extension of this work to compute form factors describing the exclusive $B \to D^{(*)}\,\tau\,\nu_\tau$ decays will deepen our understanding towards the topical $R(D^{(*)})$ puzzles, referring to the $2\,\sigma$ ($2.7\,\sigma$) deviations of the measured ratios of the corresponding branching fractions in muon and tauon channels. Such computations will enable us to pin down perturbative uncertainties in the tree-level predictions of $B \to D^{(*)}$

[7] The new technique developed in [69] using exact conformal symmetry of QCD at the critical point would be powerful in this respect.

form factors [70] and also allow for a better comparison of LCSR and heavy-quark expansion in a different testing ground. A complete discussion of radiative corrections to $B \to D^{(*)}$ form factors from the B-meson LCSR including a proper treatment of the charm-quark mass will be presented elsewhere. Third, the techniques discussed in this work can be applied to compute $\Lambda_b \to p, \Lambda$ transition form factors from the sum rules with the Λ_b-baryon DAs [71,72], which are of phenomenological interest for an alternative determination of $|V_{ub}|$ exclusively and for a complementary search of physics beyond the Standard Model. However, one should be aware of the fact that constructing baryonic sum rules are more involved than the mesonic counterpart due to various ways to choose baryonic interpolating currents and potential contaminations from negative-parity baryons in the hadronic dispersion relations [73]. To summarize, we foresee straightforward extensions of this work into different directions.

Acknowledgements

We are grateful to M. Beneke, N. Offen and J. Rohrwild for illuminating discussions, to M. Beneke for many valuable comments on the manuscript, and to D.P. Du for providing us with the Lattice data points in [55]. YMW is supported in part by the Gottfried Wilhelm Leibniz programme of the Deutsche Forschungsgemeinschaft (DFG).

Appendix A. Loop integrals

In this appendix, we collect some useful one-loop integrals in our calculations.

$$\begin{aligned} I_0 &= \int [d\,l] \frac{1}{[(p-k+l)^2+i0][l^2+2m_b\,v\cdot l+i0]} \\ &= \frac{1}{\epsilon} + 2\ln\frac{\mu}{m_b} + \frac{r}{\bar r}\ln r + 2\,, \end{aligned} \tag{111}$$

$$\begin{aligned} I_1^h &= \int [d\,l] \frac{1}{[l^2+n\cdot p\,\bar n\cdot l+i0][l^2+2m_b\,v\cdot l+i0][l^2+i0]} \\ &= \frac{-1}{2m_b\,n\cdot p}\left[\frac{1}{\epsilon^2} + \frac{2}{\epsilon}\ln\frac{\mu}{n\cdot p} + 2\ln^2\frac{\mu}{n\cdot p} - \ln^2 r - 2\,\mathrm{Li}_2\left(-\frac{\bar r}{r}\right) + \frac{\pi^2}{12}\right], \end{aligned} \tag{112}$$

$$\begin{aligned} I_1^{hc} &= \int \frac{d^D\,l}{(2\pi)^D} \frac{1}{[n\cdot(p+l)\,\bar n\cdot(p-k+l)+l_\perp^2+i0][n\cdot l+i0][l^2+i0]} \\ &= \frac{1}{n\cdot p}\left[\frac{1}{\epsilon^2} + \frac{1}{\epsilon}\ln\frac{\mu^2}{n\cdot p\,(\omega-\bar n\cdot p)} + \frac{1}{2}\ln^2\frac{\mu^2}{n\cdot p\,(\omega-\bar n\cdot p)} - \frac{\pi^2}{12}\right], \end{aligned} \tag{113}$$

$$\begin{aligned} I_{1\,\mu} &= \int [d\,l] \frac{l_\mu}{[(p-k+l)^2+i0][l^2+2m_b\,v\cdot l+i0][l^2+i0]} \\ &\equiv C_1\,(p-k)_\mu + C_2\,m_b\,v_\mu\,, \end{aligned} \tag{114}$$

$$C_1^h = -\frac{1}{m_b^2 r}\left[\frac{1}{\epsilon} + 2\ln\frac{\mu}{m_b} - \frac{r-2}{r-1}\ln r + 2\right], \tag{115}$$

$$C_2 = C_2^h = -\frac{1}{m_b^2\,\bar r}\ln r\,, \tag{116}$$

$$C_1^{hc} = C_1 - C_1^h = \frac{1}{m_b^2 r}\left[\frac{1}{\epsilon} + \ln\frac{\mu^2}{n\cdot p\,(\omega-\bar n\cdot p)} + 2\right], \tag{117}$$

$$I_{1,a} = \int [d\,l] \frac{n\cdot l\ \bar{n}\cdot l}{[(p-k+l)^2+i0][l^2+2m_b\,v\cdot l+i0][l^2+i0]}$$
$$= \frac{1}{2}\left[\frac{1}{\epsilon}+2\,\ln\frac{\mu}{m_b}+\frac{r}{\bar{r}}\,\ln r+2\right], \tag{118}$$

$$I_{1,b} = \int [d\,l] \frac{(\bar{n}\cdot l)^2}{[(p-k+l)^2+i0][l^2+2m_b\,v\cdot l+i0][l^2+i0]}$$
$$= -\frac{1}{2\,\bar{r}^2}\,[r\,\ln r+\bar{r}]\,, \tag{119}$$

$$I_2 = \int [d\,l]\,\frac{l_\alpha\ (p-l)_\beta}{[(p-l)^2+i0][(l-k)^2+i0][l^2+i0]}$$
$$\equiv -\frac{g_{\alpha\beta}}{2}\,I_{2,a} - \frac{1}{p^2}\left[k_\alpha\,k_\beta\,I_{2,b} - p_\alpha\,p_\beta\,I_{2,c} - k_\alpha\,p_\beta\,I_{2,d} + p_\alpha\,k_\beta\,I_{2,e}\right], \tag{120}$$

$$I_{2,a} = \frac{1}{2}\left[\frac{1}{\epsilon}+\ln\left(-\frac{\mu^2}{p^2}\right)-\frac{1+\eta}{\eta}\,\ln(1+\eta)+3\right], \tag{121}$$

$$I_{2,b} = \frac{2\,\eta-\eta^2-2\,\ln(1+\eta)}{2\,\eta^3}\left[\frac{1}{\epsilon}+\ln\left(-\frac{\mu^2}{p^2}\right)-\ln(1+\eta)+3\right]$$
$$+\frac{\eta^2-\ln^2(1+\eta)}{2\,\eta^3}\,, \tag{122}$$

$$I_{2,c} = \frac{\ln(1+\eta)}{2\,\eta}\,, \tag{123}$$

$$I_{2,d} = \frac{\ln(1+\eta)-\eta}{\eta^2}\left[\frac{1}{\epsilon}+\ln\left(-\frac{\mu^2}{p^2}\right)-\ln(1+\eta)+\frac{5}{2}\right]+\frac{\ln^2(1+\eta)}{2\,\eta^2}\,, \tag{124}$$

$$I_{2,e} = \frac{\eta-\ln(1+\eta)}{2\,\eta^2}\,, \tag{125}$$

$$I_3 = \int [d\,l]\frac{1}{[(p-k+l)^2+i0][l^2+i0]} = \frac{1}{\epsilon}+\ln\frac{\mu^2}{n\cdot p\,\bar{n}\cdot(k-p)}+2\,, \tag{126}$$

$$I_{3\,\mu} = \int [d\,l]\frac{l_\mu}{[(p-k+l)^2+i0][l^2+i0]} = -\frac{I_3}{2}\,(p-k)_\mu\,, \tag{127}$$

$$I_{4,a} = \int \frac{d^D\,l}{(2\pi)^D}\,\frac{n\cdot(p+l)}{[n\cdot(p+l)\,\bar{n}\cdot(p-k+l)+l_\perp^2+i0][n\cdot l\,\bar{n}(l-k)+l_\perp^2+i0][l^2+i0]}$$
$$= \frac{\ln(1+\eta)}{\omega}\left[\frac{1}{\epsilon}+\ln\frac{\mu^2}{n\cdot p\,(\omega-\bar{n}\cdot p)}+\frac{1}{2}\,\ln(1+\eta)+1\right], \tag{128}$$

$$I_{4,b} = \int \frac{d^D\,l}{(2\pi)^D}\,\frac{n\cdot l\ n\cdot(p+l)}{[n\cdot(p+l)\,\bar{n}\cdot(p-k+l)+l_\perp^2+i0][n\cdot l\,\bar{n}(l-k)+l_\perp^2+i0][l^2+i0]}$$
$$= \frac{n\cdot p}{2\,\omega}\,\ln(1+\eta)\,, \tag{129}$$

with $r = n\cdot p/m_b$, $\bar{r} = 1-r$, $\omega = \bar{n}\cdot k$ and $\eta = -\omega/\bar{n}\cdot p$.

Appendix B. Spectral representations

We collect the spectral functions of convolution integrals entering the factorization formulae of Π and $\widetilde{\Pi}$ in (73). These expressions were first derived in [4], we confirmed these spectral functions independently and also verified the corresponding dispersion integrals.

$$\frac{1}{\pi}\,\mathrm{Im}_{\omega'}\int_0^\infty \frac{d\omega}{\omega}\,\ln\frac{\omega'-\omega}{\omega'}\,\phi_B^+(\omega,\mu)=\int_{\omega'}^\infty \frac{d\omega}{\omega}\,\phi_B^+(\omega,\mu)\,, \tag{130}$$

$$\begin{aligned}&\frac{1}{\pi}\,\mathrm{Im}_{\omega'}\int_0^\infty \frac{d\omega}{\omega-\omega'-i0}\,\ln^2\frac{\mu^2}{n\cdot p\,(\omega-\omega')}\,\phi_B^-(\omega,\mu)\\&\quad=\int_0^\infty d\omega\left[\frac{2\,\theta(\omega'-\omega)}{\omega-\omega'}\,\ln\frac{\mu^2}{n\cdot p\,(\omega'-\omega)}\right]_\oplus\phi_B^-(\omega,\mu)+\left[\ln^2\frac{\mu^2}{n\cdot p\,\omega'}-\frac{\pi^2}{3}\right],\end{aligned} \tag{131}$$

$$\begin{aligned}&\frac{1}{\pi}\,\mathrm{Im}_{\omega'}\int_0^\infty \frac{d\omega}{\omega-\omega'-i0}\,\ln^2\frac{\omega'-\omega}{\omega'}\,\phi_B^-(\omega,\mu)\\&\quad=-\int_{\omega'}^\infty d\omega\left[\ln^2\frac{\omega-\omega'}{\omega'}-\frac{\pi^2}{3}\right]\frac{d}{d\omega}\phi_B^-(\omega,\mu)\,,\end{aligned} \tag{132}$$

$$\begin{aligned}&\frac{1}{\pi}\,\mathrm{Im}_{\omega'}\int_0^\infty \frac{d\omega}{\omega-\omega'-i0}\,\ln\frac{\omega'-\omega}{\omega'}\,\ln\frac{\mu^2}{n\cdot p\,(\omega-\omega')}\,\phi_B^-(\omega,\mu)\\&\quad=\int_0^\infty d\omega\left[\frac{\theta(\omega'-\omega)}{\omega-\omega'}\,\ln\frac{\omega'-\omega}{\omega'}\right]_\oplus\phi_B^-(\omega,\mu)\\&\qquad+\frac{1}{2}\int_{\omega'}^\infty d\omega\left[\ln^2\frac{\mu^2}{n\cdot p\,(\omega-\omega')}-\ln^2\frac{\mu^2}{n\cdot p\,\omega'}+\frac{\pi^2}{3}\right]\frac{d}{d\omega}\phi_B^-(\omega,\mu)\,,\end{aligned} \tag{133}$$

$$\begin{aligned}&\frac{1}{\pi}\,\mathrm{Im}_{\omega'}\int_0^\infty \frac{d\omega}{\omega-\omega'-i0}\,\ln\frac{\omega'-\omega}{\omega'}\,\phi_B^-(\omega,\mu)\\&\quad=-\int_{\omega'}^\infty d\omega\,\ln\frac{\omega-\omega'}{\omega'}\,\frac{d}{d\omega}\phi_B^-(\omega,\mu)\,.\end{aligned} \tag{134}$$

Appendix C. Two-point QCD sum rules for f_B and f_π

For completeness, we collect the two-point sum rules for the B-meson decay constant f_B in QCD [51,74] including NLO corrections to the perturbative term and to the $D=3$ quark condensate part:

$$f_B^2 = \frac{e^{m_B^2/\overline{M}^2}\, m_b^2}{m_B^4}\left\{\int_{m_b^2}^{\bar{s}_0} ds\, e^{-s/\overline{M}^2}\, \frac{3}{8\pi^2}\left[\frac{(s-m_b^2)^2}{s} + \frac{\alpha_s\, C_F}{\pi}\,\rho_{pert}^{(1)}(s,m_b^2)\right]\right.$$
$$+ e^{-m_b^2/\overline{M}^2}\left[-m_b\,\langle\bar{q}q\rangle\left(1+\frac{\alpha_s\, C_F}{\pi}\,\rho_{q\bar{q}}^{(1)}(s,m_b^2)\right) - \frac{m_b\langle\bar{q}Gq\rangle}{2\,\overline{M}^2}\left(1-\frac{m_b^2}{2\overline{M}^2}\right)\right.$$
$$\left.\left. + \frac{1}{12}\left\langle\frac{\alpha_s}{\pi}GG\right\rangle - \frac{16\pi}{27}\,\frac{\alpha_s\langle\bar{q}q\rangle^2}{\overline{M}^2}\left(1-\frac{m_b^2}{4\,\overline{M}^2}-\frac{m_b^4}{12\,\overline{M}^4}\right)\right]\right\}, \tag{135}$$

where $\overline{M}^2$ and $\bar{s}_0$ are the Borel parameter and the effective threshold, and the relevant NLO spectral functions are given by

$$\rho_{pert}^{(1)}(s,m_b^2) = \frac{\bar{x}\,s}{2}\left\{\bar{x}\,[4\,\mathrm{Li}_2(x) + 2\,\ln x\,\ln\bar{x} - (5-2x)\,\ln\bar{x}]\right.$$
$$\left. + (1-2x)\,(3-x)\,\ln x + 3\,(1-3x)\,\ln\frac{\mu^2}{m_b^2} + \frac{17-33x}{2}\right\}, \tag{136}$$

$$\rho_{q\bar{q}}^{(1)}(s,m_b^2) = -\frac{3}{2}\left[\Gamma\left(0,\frac{m_b^2}{\overline{M}^2}\right)e^{m_b^2/\overline{M}^2} - \left(1-\frac{m_b^2}{\overline{M}^2}\left(\ln\frac{\mu^2}{m_b^2}+\frac{4}{3}\right)\right) - 1\right], \tag{137}$$

with $x = m_b^2/s$, $\bar{x} = 1-x$ and the incomplete Γ function defined as

$$\Gamma(n,x) = \int_x^\infty dt\;\; t^{n-1}\,e^{-t}. \tag{138}$$

The two-point QCD sum rules of the pion decay constant f_π including the perturbative term at $\mathcal{O}(\alpha_s)$ reads [75]

$$f_\pi^2 = M^2\left[\frac{1}{4\pi^2}\left(1-e^{-s_0/M^2}\right)\left(1+\frac{\alpha_s(M)}{\pi}\right) + \frac{1}{12\,M^4}\left\langle\frac{\alpha_s}{\pi}GG\right\rangle\right.$$
$$\left. + \frac{176\pi}{81}\,\frac{\alpha_s\langle\bar{q}q\rangle^2}{M^6}\right]. \tag{139}$$

References

[1] A. Khodjamirian, T. Mannel, N. Offen, Phys. Lett. B 620 (2005) 52, arXiv:hep-ph/0504091.
[2] A. Khodjamirian, T. Mannel, N. Offen, Phys. Rev. D 75 (2007) 054013, arXiv:hep-ph/0611193.
[3] F. De Fazio, T. Feldmann, T. Hurth, Nucl. Phys. B 733 (2006) 1;
F. De Fazio, T. Feldmann, T. Hurth, Nucl. Phys. B 800 (2008) 405, arXiv:hep-ph/0504088.
[4] F. De Fazio, T. Feldmann, T. Hurth, J. High Energy Phys. 0802 (2008) 031, arXiv:0711.3999 [hep-ph].
[5] M. Beneke, V.A. Smirnov, Nucl. Phys. B 522 (1998) 321, arXiv:hep-ph/9711391.
[6] P. Ball, R. Zwicky, J. High Energy Phys. 0110 (2001) 019, arXiv:hep-ph/0110115.
[7] P. Ball, R. Zwicky, Phys. Rev. D 71 (2005) 014015, arXiv:hep-ph/0406232.
[8] G. Duplancic, A. Khodjamirian, T. Mannel, B. Melic, N. Offen, J. High Energy Phys. 0804 (2008) 014, arXiv:0801.1796 [hep-ph].
[9] A. Bharucha, J. High Energy Phys. 1205 (2012) 092, arXiv:1203.1359 [hep-ph].
[10] M. Beneke, T. Feldmann, Nucl. Phys. B 592 (2001) 3, arXiv:hep-ph/0008255.
[11] C.W. Bauer, S. Fleming, D. Pirjol, I.W. Stewart, Phys. Rev. D 63 (2001) 114020, arXiv:hep-ph/0011336.
[12] M. Beneke, Y. Kiyo, D.S. Yang, Nucl. Phys. B 692 (2004) 232, arXiv:hep-ph/0402241.

[13] T. Becher, R.J. Hill, J. High Energy Phys. 0410 (2004) 055, arXiv:hep-ph/0408344.
[14] R. Bonciani, A. Ferroglia, J. High Energy Phys. 0811 (2008) 065, arXiv:0809.4687 [hep-ph].
[15] H.M. Asatrian, C. Greub, B.D. Pecjak, Phys. Rev. D 78 (2008) 114028, arXiv:0810.0987 [hep-ph].
[16] M. Beneke, T. Huber, X.-Q. Li, Nucl. Phys. B 811 (2009) 77, arXiv:0810.1230 [hep-ph].
[17] G. Bell, Nucl. Phys. B 812 (2009) 264, arXiv:0810.5695 [hep-ph].
[18] G. Bell, M. Beneke, T. Huber, X.Q. Li, Nucl. Phys. B 843 (2011) 143, arXiv:1007.3758 [hep-ph].
[19] R.J. Hill, T. Becher, S.J. Lee, M. Neubert, J. High Energy Phys. 0407 (2004) 081, arXiv:hep-ph/0404217.
[20] M. Beneke, D.S. Yang, Nucl. Phys. B 736 (2006) 34, arXiv:hep-ph/0508250.
[21] M. Beneke, T. Feldmann, Nucl. Phys. B 685 (2004) 249, arXiv:hep-ph/0311335.
[22] J.C. Collins, Adv. Ser. Dir. High Energy Phys. 5 (1989) 573, arXiv:hep-ph/0312336.
[23] J. Botts, G.F. Sterman, Nucl. Phys. B 325 (1989) 62.
[24] H.n. Li, Y.L. Shen, Y.M. Wang, Phys. Rev. D 85 (2012) 074004, arXiv:1201.5066 [hep-ph].
[25] H.N. Li, Y.L. Shen, Y.M. Wang, J. High Energy Phys. 1302 (2013) 008, arXiv:1210.2978 [hep-ph];
Y.L. Shen, Y.M. Wang, EPJ Web Conf. 80 (2014) 00047, arXiv:1409.1048 [hep-ph].
[26] S. Cheng, Y.Y. Fan, X. Yu, C.D. Lü, Z.J. Xiao, Phys. Rev. D 89 (9) (2014) 094004, arXiv:1402.5501 [hep-ph].
[27] H.n. Li, Y.M. Wang, arXiv:1410.7274 [hep-ph];
Y.M. Wang, Int. J. Mod. Phys. Conf. Ser. 37 (2015) 1560049.
[28] A.G. Grozin, M. Neubert, Phys. Rev. D 55 (1997) 272, arXiv:hep-ph/9607366.
[29] M. Beneke, J. Rohrwild, Eur. Phys. J. C 71 (2011) 1818, arXiv:1110.3228 [hep-ph].
[30] S. Descotes-Genon, C.T. Sachrajda, Nucl. Phys. B 650 (2003) 356, arXiv:hep-ph/0209216.
[31] S.W. Bosch, R.J. Hill, B.O. Lange, M. Neubert, Phys. Rev. D 67 (2003) 094014, arXiv:hep-ph/0301123.
[32] G. Bell, T. Feldmann, J. High Energy Phys. 0804 (2008) 061, arXiv:0802.2221 [hep-ph].
[33] S. Descotes-Genon, N. Offen, J. High Energy Phys. 0905 (2009) 091, arXiv:0903.0790 [hep-ph].
[34] B.O. Lange, M. Neubert, Phys. Rev. Lett. 91 (2003) 102001, arXiv:hep-ph/0303082.
[35] G. Bell, T. Feldmann, Y.M. Wang, M.W.Y. Yip, J. High Energy Phys. 1311 (2013) 191, arXiv:1308.6114 [hep-ph].
[36] V.M. Braun, A.N. Manashov, Phys. Lett. B 731 (2014) 316, arXiv:1402.5822 [hep-ph].
[37] S.J. Lee, M. Neubert, Phys. Rev. D 72 (2005) 094028, arXiv:hep-ph/0509350.
[38] T. Feldmann, B.O. Lange, Y.M. Wang, Phys. Rev. D 89 (11) (2014) 114001, arXiv:1404.1343 [hep-ph].
[39] V.M. Braun, D.Y. Ivanov, G.P. Korchemsky, Phys. Rev. D 69 (2004) 034014, arXiv:hep-ph/0309330.
[40] K.A. Olive, et al., Particle Data Group, Chin. Phys. C 38 (2014) 090001.
[41] A. Khodjamirian, T. Mannel, A.A. Pivovarov, Y.-M. Wang, J. High Energy Phys. 1009 (2010) 089, arXiv:1006.4945 [hep-ph].
[42] K.G. Chetyrkin, J.H. Kuhn, A. Maier, P. Maierhofer, P. Marquard, M. Steinhauser, C. Sturm, Phys. Rev. D 80 (2009) 074010, arXiv:0907.2110 [hep-ph].
[43] M. Beneke, A. Maier, J. Piclum, T. Rauh, Nucl. Phys. B 891 (2015) 42, arXiv:1411.3132 [hep-ph].
[44] B. Dehnadi, A.H. Hoang, V. Mateu, arXiv:1504.07638 [hep-ph].
[45] M. Beneke, M. Neubert, Nucl. Phys. B 675 (2003) 333, arXiv:hep-ph/0308039.
[46] M. Beneke, S. Jager, Nucl. Phys. B 768 (2007) 51, arXiv:hep-ph/0610322.
[47] A. Heller, et al., Belle Collaboration, arXiv:1504.05831 [hep-ex].
[48] A. Khodjamirian, T. Mannel, N. Offen, Y.-M. Wang, Phys. Rev. D 83 (2011) 094031, arXiv:1103.2655 [hep-ph].
[49] I.S. Imsong, A. Khodjamirian, T. Mannel, D. van Dyk, J. High Energy Phys. 1502 (2015) 126, arXiv:1409.7816 [hep-ph].
[50] R.J. Hill, Phys. Rev. D 73 (2006) 014012, arXiv:hep-ph/0505129.
[51] P. Gelhausen, A. Khodjamirian, A.A. Pivovarov, D. Rosenthal, Phys. Rev. D 88 (2013) 014015, Phys. Rev. D 89 (2014) 099901, arXiv:1305.5432 [hep-ph].
[52] S. Aoki, Y. Aoki, C. Bernard, T. Blum, G. Colangelo, M. Della Morte, S. Drr, A.X. El Khadra, et al., Eur. Phys. J. C 74 (2014) 2890, arXiv:1310.8555 [hep-lat].
[53] C. Bourrely, I. Caprini, L. Lellouch, Phys. Rev. D 79 (2009) 013008;
C. Bourrely, I. Caprini, L. Lellouch, Phys. Rev. D 82 (2010) 099902, arXiv:0807.2722 [hep-ph].
[54] R.J. Hill, G. Paz, Phys. Rev. D 82 (2010) 113005, arXiv:1008.4619 [hep-ph].
[55] J.A. Bailey, et al., Fermilab Lattice and MILC Collaborations, arXiv:1503.07839 [hep-lat].
[56] E. Dalgic, A. Gray, M. Wingate, C.T.H. Davies, G.P. Lepage, J. Shigemitsu, Phys. Rev. D 73 (2006) 074502, Phys. Rev. D 75 (2007) 119906, arXiv:hep-lat/0601021.
[57] J.M. Flynn, T. Izubuchi, T. Kawanai, C. Lehner, A. Soni, R.S. Van de Water, O. Witzel, Phys. Rev. D 91 (7) (2015) 074510, arXiv:1501.05373 [hep-lat].
[58] J.P. Lees, et al., BaBar Collaboration, Phys. Rev. D 86 (2012) 092004, arXiv:1208.1253 [hep-ex].

[59] A. Sibidanov, et al., Belle Collaboration, Phys. Rev. D 88 (3) (2013) 032005, arXiv:1306.2781 [hep-ex].
[60] P. del Amo Sanchez, et al., BaBar Collaboration, Phys. Rev. D 83 (2011) 032007, arXiv:1005.3288 [hep-ex].
[61] P. del Amo Sanchez, et al., BaBar Collaboration, Phys. Rev. D 83 (2011) 052011, arXiv:1010.0987 [hep-ex].
[62] H. Ha, et al., Belle Collaboration, Phys. Rev. D 83 (2011) 071101, arXiv:1012.0090 [hep-ex].
[63] B.O. Lange, Eur. Phys. J. C 33 (2004) S324;
B.O. Lange, Nucl. Phys. B, Proc. Suppl. 133 (2004) 174, arXiv:hep-ph/0310139.
[64] P. Ball, arXiv:hep-ph/0308249.
[65] A. Hardmeier, E. Lunghi, D. Pirjol, D. Wyler, Nucl. Phys. B 682 (2004) 150, arXiv:hep-ph/0307171.
[66] Y.C. Chen, H.N. Li, Phys. Lett. B 712 (2012) 63, arXiv:1112.5059 [hep-ph].
[67] M. Knodlseder, N. Offen, J. High Energy Phys. 1110 (2011) 069, arXiv:1105.4569 [hep-ph].
[68] V.M. Braun, A.N. Manashov, J. Rohrwild, Nucl. Phys. B 826 (2010) 235, arXiv:0908.1684 [hep-ph].
[69] V.M. Braun, A.N. Manashov, Phys. Lett. B 734 (2014) 137, arXiv:1404.0863 [hep-ph].
[70] S. Faller, A. Khodjamirian, C. Klein, T. Mannel, Eur. Phys. J. C 60 (2009) 603, arXiv:0809.0222 [hep-ph].
[71] Y.M. Wang, Y.L. Shen, C.D. Lü, Phys. Rev. D 80 (2009) 074012, arXiv:0907.4008 [hep-ph].
[72] T. Feldmann, M.W.Y. Yip, Phys. Rev. D 85 (2012) 014035;
T. Feldmann, M.W.Y. Yip, Phys. Rev. D 86 (2012) 079901, arXiv:1111.1844 [hep-ph].
[73] A. Khodjamirian, C. Klein, T. Mannel, Y.-M. Wang, J. High Energy Phys. 1109 (2011) 106, arXiv:1108.2971 [hep-ph].
[74] M. Jamin, B.O. Lange, Phys. Rev. D 65 (2002) 056005, arXiv:hep-ph/0108135.
[75] P. Colangelo, A. Khodjamirian, in: M. Shifman (Ed.), At the Frontier of Particle Physics, vol. 3, 2000, pp. 1495–1576, arXiv:hep-ph/0010175.